

คอมพอสิตของแกรฟีนออกไซด์และอนุภาคเงินระดับนาโนเมตร
ที่กระจายตัวได้ดีในตัวทำละลายอินทรีย์



นางสาวอรพร วงษ์อุระ

จุฬาลงกรณ์มหาวิทยาลัย

CHULALONGKORN UNIVERSITY

บทคัดย่อและแฟ้มข้อมูลฉบับเต็มของวิทยานิพนธ์ตั้งแต่ปีการศึกษา 2554 ที่ให้บริการในคลังปัญญาจุฬาฯ (CUIR)
เป็นแฟ้มข้อมูลของนิสิตเจ้าของวิทยานิพนธ์ ที่ส่งผ่านทางบัณฑิตวิทยาลัย

The abstract and full text of theses from the academic year 2011 in Chulalongkorn University Intellectual Repository (CUIR)
are the thesis authors' files submitted through the University Graduate School.

วิทยานิพนธ์นี้เป็นส่วนหนึ่งของการศึกษาตามหลักสูตรปริญญาวิทยาศาสตรมหาบัณฑิต

สาขาวิชาปิโตรเคมีและวิทยาศาสตร์พอลิเมอร์

คณะวิทยาศาสตร์ จุฬาลงกรณ์มหาวิทยาลัย

ปีการศึกษา 2559

ลิขสิทธิ์ของจุฬาลงกรณ์มหาวิทยาลัย

HIGHLY DISPERSED GRAPHENE OXIDE-
SILVER NANOPARTICLE COMPOSITES IN ORGANIC SOLVENTS

Miss Oraporn Wong-u-ra



A Thesis Submitted in Partial Fulfillment of the Requirements
for the Degree of Master of Science Program in Petrochemistry and Polymer Science

Faculty of Science

Chulalongkorn University

Academic Year 2016

Copyright of Chulalongkorn University

อรพร วงษ์อุระ : คอมพอสิตของแกรฟีนออกไซด์และอนุภาคเงินระดับนาโนเมตรที่กระจายตัวได้ดีในตัวทำละลายอินทรีย์ (HIGHLY DISPERSED GRAPHENE OXIDE-SILVER NANOPARTICLE COMPOSITES IN ORGANIC SOLVENTS) อ.ที่ปรึกษาวิทยานิพนธ์หลัก: ผศ. ดร. คณศ วงษ์ระวี, 56 หน้า.

งานวิจัยนี้ได้นำเสนอและพัฒนากระบวนการเคลื่อนย้ายอนุภาคเงินระดับนาโนเมตรจากชั้นน้ำไปยังชั้นตัวทำละลายอินทรีย์ โดยอาศัยแกรฟีนออกไซด์เป็นวัสดุตัวพา แบ่งขั้นตอนการทดลองออกเป็น 2 ขั้นตอน ขั้นแรกคือ การสังเคราะห์คอมพอสิตระหว่างแกรฟีนออกไซด์และอนุภาคเงินระดับนาโนเมตร (GO/AgNP composites) ซึ่งจะสังเคราะห์อนุภาคเงินระดับนาโนเมตรผ่านปฏิกิริยารีดักชันในสารแขวนลอยแกรฟีนออกไซด์ โดยมีไดเมทิลฟอร์มาไมด์เป็นตัวรีดิวซ์ และอนุภาคเงินระดับนาโนเมตรที่ได้นั้นจะถูกทำให้มีความเสถียรด้วยหมู่ฟังก์ชันที่มีออกซิเจนเป็นองค์ประกอบบนแกรฟีนออกไซด์ผ่านอันตรกิริยาไฟฟ้าสถิต จากนั้นคอมพอสิตถูกตรวจสอบลักษณะเฉพาะและทดสอบความบริสุทธิ์ด้วยเทคนิคดังนี้ ยูวีวิสิเบิลสเปกโทรสโกปี ฟลูออโรสเปกโทรสโกปี เทคนิคการเลี้ยวเบนของรังสีเอ็กซ์แบบผง รามานสเปกโทรสโกปี เทคนิคกล้องจุลทรรศน์อิเล็กตรอนแบบส่องผ่าน เทคนิคกล้องจุลทรรศน์อิเล็กตรอนแบบส่องกราดและเทคนิคการกระจายพลังงานของรังสีเอ็กซ์ ส่วนขั้นที่สองคือ การดัดแปรพื้นผิวของแกรฟีนออกไซด์ด้วยแอลคิลเอมีน โดยแอลคิลเอมีนที่เลือกใช้คือ โอลิวลามีน เพื่อช่วยเพิ่มคุณสมบัติความไม่ชอบน้ำ ทำให้คอมพอสิตกระจายตัวได้ดีในตัวทำละลายอินทรีย์ 6 ชนิดดังนี้ โทลูอีน บิวทานอล ไอโซบิวทิลแอลกอฮอล์ เอทิลแอลกอฮอล์ อะซีโตน ไตรคลอโรเอทิลีน ไกลคอล เนื่องจากสมบัติของตัวทำละลายอินทรีย์ที่แตกต่างกัน จึงมีความจำเป็นที่จะต้องหาปริมาณของโอลิวลามีนที่เหมาะสมในตัวทำละลายอินทรีย์แต่ละชนิด หลังจากนั้นจะดัดแปรพื้นผิวของคอมพอสิตด้วยปริมาณโอลิวลามีนที่เหมาะสม เพื่อให้คอมพอสิตสามารถกระจายตัวได้ในชั้นตัวทำละลายอินทรีย์ จากการทดลองพบว่า คอมพอสิตมีประสิทธิภาพในการกระจายตัวที่ดีในตัวทำละลายอินทรีย์หลังจากการโซนิกเคชันเป็นเวลาอย่างน้อย 6 ชั่วโมง กระบวนการที่พัฒนานี้ไม่ซับซ้อนและให้ประสิทธิภาพสูงในการเคลื่อนย้ายอนุภาคเงินระดับนาโนเมตรไปยังชั้นตัวทำละลายอินทรีย์

สาขาวิชา ปีเตอร์เคมีและวิทยาศาสตร์พอลิเมอร์ ลายมือชื่อนิสิต

ปีการศึกษา 2559

ลายมือชื่อ อ.ที่ปรึกษาหลัก

5772209823 : MAJOR PETROCHEMISTRY AND POLYMER SCIENCE

KEYWORDS: GRAPHENE OXIDE / SILVER NANOPARTICLE

ORAPORN WONG- U- RA: HIGHLY DISPERSED GRAPHENE OXIDE- SILVER NANOPARTICLE COMPOSITES IN ORGANIC SOLVENTS. ADVISOR: ASST. PROF. KANET WONGRAVEE, Ph.D., 56 pp.

An innovative phase transfer process of anisotropic silver nanoparticles (AgNPs) from water to a wide range of organic solvents such as toluene, n-butanol, iso-butyl acetate, ethyl acetate, acetonitrile and ethylene glycol was described. In the developed process, AgNPs were transferred to the organic solvents by using the graphene oxide (GO) sheets as the carrier. The transferring process was utilized by two straightforward steps. Firstly, AgNPs were synthesized using *N-N'* dimethylformamide (DMF) as a reducing agent and they were stabilized by the numerous of oxygen-functional groups on the GO surface via electrostatic interaction to form GO/AgNP composites. The existence, purity and stability of AgNPs on the GO sheets were examined and analyzed by several techniques such as UV-Visible spectroscopy (UV-Vis), Fourier-transform Infrared (FT-IR) spectroscopy, Raman spectroscopy, X-ray powder diffraction (XRD), transmission electron microscopy (TEM), scanning electron microscopy (SEM) and energy-dispersive X-ray spectroscopy (EDX). Secondly, the GO/AgNP composites were modified with oleylamine (OAm) in order to improve hydrophobicity. To obtain the maximum phase transfer efficiency, an appropriate amount of OAm was carefully optimized for each organic solvent. The dispersion behavior of the GO/AgNP composites modified with OAm (GO/AgNP-OAm) in the organic solvents were investigated. It was found that the GO/AgNP-OAm are uniformly dispersed in the organic solvents for at least 6 hours after sonication. The developed phase transfer method has the features of simplicity and high efficiency.

Field of Study: Petrochemistry and
Polymer Science

Student's Signature

Advisor's Signature

Academic Year: 2016

ACKNOWLEDGEMENTS

I would like to extend my sincere gratitude to all people who have helped and inspired me with their abilities. This thesis has been successfully completed with their kind supporting.

First of all, I would like to express my deepest appreciation to my advisor, Assistant Professor Dr. Kanet Wongravee who has been the sustained source of the enthusiasm during the whole time of my master program. I am also indebted to him for his endless guidance and inspiring suggestions throughout my research. Furthermore, he is a reachable person who always gives the powerful encouragement and advises the smart ideas not only for his students, but also the others. Fortunately, I am one of his advisees.

I would like to express my gratitude to Professor Dr. Sanong Ekgasit, Associate Professor Chuchaat Thammacharoen for the useful theoretical background and the improvement of presentation skills.

I would like to sincerely appreciation Associate Professor Dr. Pranut Potiyaraj, Dr. Prompong Pienpinijtham and Dr. Chaval Sriwong who devote their time for being my thesis committee and give me the useful suggestion.

I would also convey my heartfelt gratefulness to all of my beloved friends, my colleagues and organization: Sensor Research Unit (SRU), Department of Chemistry, Faculty of science, Chulalongkorn University for warm-hearted and spiritual supporting during this research. Because of their constant encouragement, this thesis would be successful. It was a good chance as I was a member of SRU group which is plentiful of kindness like family. In particular, Dr. Harnchana Gatemala who suggests the alternative ways for planning of my experiments, reviewing this thesis and always lighten me with his joke as well as Miss Thanyada Sukmanee for revision this thesis.

Finally, I deeply appreciate my family for the unconditional love to me. No words are enough to thank you for their encouragement which pushes me through the success. It is my fortune to be your daughter with the great parents.

CONTENTS

	Page
THAI ABSTRACT	iv
ENGLISH ABSTRACT	v
ACKNOWLEDGEMENTS	vi
CONTENTS	vii
LIST OF TABLES	ix
LIST OF FIGURES	xi
ABBREVIATIONS.....	xiv
CHAPTER 1 INTRODUCTION.....	1
1.1 The objectives	9
1.2 Scopes of this research	9
CHAPTER 2 THEORETICAL BACKGROUND.....	10
2.1 Silver nanoparticles (AgNPs).....	10
2.2 Phase transfer method in metal nanoparticles (MNPs).....	12
2.3 Graphene oxide (GO)	15
2.4 Phase transfer of GO into organic solvents	17
2.5 The metal on graphene/GO surface	18
CHAPTER 3 EXPERIMENTS.....	19
3.1 Chemicals and Materials.....	19
3.2 Instruments	20
3.3 The synthesis of graphene oxide-silver nanoparticle (GO/AgNP) composites....	20
3.4 The optimization amount of OAm for transferring GO to organic solvents.....	22
3.5 The GO/AgNPs-OAm composite in organic solvents	24

	Page
3.6 Characterization	25
CHAPTER 4 RESULTS AND DISCUSSION	26
4.1 The synthesis of GO/AgNP composites	26
4.2 The optimization amount of OAm for transferring GO to organic solvents.....	34
4.3 Phase transferring GO/AgNP composites to organic solvents	42
CHAPTER 5 CONCLUSIONS	48
REFERENCES	49
VITA.....	56



LIST OF TABLES

	Page
Table 1. 1 Physical, chemical and photochemical methods synthesis and stabilize AgNPs.....	1
Table 1. 2 The phase transfer of AgNPs into organic solvents by using various ligands.	3
Table 1. 3 The preparation of GO/AgNP composites.....	8
Table 4. 1 The equations and R^2 values at different wavelength.....	36
Table 4. 2 The physical properties of DI water and organic solvents.....	37



LIST OF FIGURES

	Page
Fig. 1. 1 Phase transfer of AgNP by using surfactant.....	4
Fig. 1. 2 Phase transfer of AgNPs by using a carrier system.....	5
Fig. 1. 3 Schematic illustration of the synthesis of graphene oxide.....	6
Fig. 1. 4 Schematic illustration of the synthesis and phase transfer process of GO/AgNP composites using OAm as a transferring agent.....	6
Fig. 2. 1 Localized surface plasmon resonance of nanoparticles.....	11
Fig. 2. 2 The anti-bacterial mechanism of AgNP.....	11
Fig. 2. 3 Schematic of the phase transfer of gold nanoparticles by Brust-Schiffring method.....	12
Fig. 2. 4 Schematic of the transferring of MNPs by “naked” nanoparticles method.....	13
Fig. 2. 5 Schematic of the transferring of MNPs into hexane by ligand exchange method.....	13
Fig. 2. 6 Schematic of the transferring of MNPs into hexane by electrostatic interaction.....	14
Fig. 2. 7 Structures of graphite, graphite oxide and graphene oxide.....	15
Fig. 2. 8 The functionalized reactions with graphene oxide.....	16
Fig. 2. 9 The modification of GO by various transfer agents.....	17
Fig. 3. 1 Schematic drawing of the preparation of GO/AgNP composites by using DMF as a reducing agent.....	21
Fig. 3. 2 Schematic illustration showing the measurement of calibration curve..	22
Fig. 3. 3 Schematic illustration of the modification of GO by using OAm for increasing hydrophobicity.....	23
Fig. 3. 4 Schematic illustration of the preparation of the GO/AgNPs-OAm dispersed in organic solvents.....	24

LIST OF FIGURES

	Page
Fig. 4. 1 UV-Vis spectra of the synthesized GO/AgNP composites at the different reaction times.....	26
Fig. 4. 2 (A) UV-Vis spectra of the AgNP (solid line) by using DMF as reducing agent and supernatant of AgNP solution after centrifuging at 2000 rpm for 10 min (dot line). (B) UV-Vis spectra of GO/AgNP composites (blue line), the original GO suspension (red line) and the supernatant of GO/AgNP composites after sonication for 30 min (green line)	28
Fig. 4. 3 TGA thermograms of the original GO suspension (red line) and the GO/AgNP composites (blue line)	29
Fig. 4. 4 Raman spectra of PATP 30mM using the GO and the GO/AgNP composites as SERS substrate.....	30
Fig. 4. 5 (A) EDX spectrum and elemental maps of GO/AgNP composites. (B) the EDX analysis on a few selected areas of the GO/AgNP composites to determine the element compositions.....	31
Fig. 4. 6 XRD patterns of the GO suspension (red line) and the GO/AgNP composites (blue line)	32
Fig. 4. 7 TEM images of (A) the original GO suspension and (B) the GO/AgNP composites. (C) Histogram of the size distribution of AgNPs on GO sheets.....	33
Fig. 4. 8 The preparation of GO/AgNP composites by using DMF as a reducing agent.....	34

LIST OF FIGURES

	Page
Fig. 4. 9 UV-Vis spectra of the GO suspension at various concentrations. The inset image represents the solution containing the dispersed GO suspensions.....	35
Fig. 4. 10 the calibration curves of the GO concentrations (10-50 ppm) and the average of absorbance at 240, 300, 360, 420, 450, 550 and 650 nm.....	36
Fig. 4. 11 (A) The chart of the dispersion activity at various weight ratio of GO-OAm in several organic solvents, (B) The dispersed GO in organic solvents and (C) Insets images represent the GO-OAm in organic solvents after sonication, after adding DI water and after adding various amount OAm.....	39
Fig. 4. 12 FT-IR spectra of the original GO suspension, the pure OAm and the GO-OAm.....	40
Fig. 4. 13 Inset digital images of the dispersed GO-OAm in organic solvents immediately after sonication and after leaving for 0-18 hours.....	41
Fig. 4. 14 (A) UV-Visible spectra and (B) normalized UV-visible spectra of the dispersion of GO/AgNPs-OAm in the organic solvents. (C) the digital images represent the dispersed GO/AgNPs-OAm in the organic solvents immediately after sonication, after adding DI water and (D) after leaving them for 0-18 hours.....	43
Fig. 4. 15 TGA thermograms of the GO-OAm composites (red line) and the GO/AgNPs-OAm (blue line)	44
Fig. 4. 16 (A, B) TEM images of GO/AgNPs-OAm in EtOAc (C) histogram of the size distribution of AgNPs on GO nanosheets in EtOAc.....	45

LIST OF FIGURES

	Page
Fig. 4. 17 UV-Vis spectra of the re-dispersed GO/AgNPs-OAm pellets (solid lines) and the supernatant (dot lines) in the organic solvents....	46
Fig. 4. 18 Inset images of the dispersed GO/AgNPs-OAm in organic solvents after immediately sonication, leaving for 6 hours, 18 hours and after re-dispersion.....	47



ABBREVIATIONS

AgNPs	silver nanoparticles
GO	graphene oxide
OAm	oleylamine
GO/AgNP	composite of graphene oxide-silver nanoparticle
GO-OAm	modified GO by OAm
GO/AgNPs-OAm	modified GO/AgNP composites by OAm
MNPs	metal nanoparticles
Ag ⁰	metallic silver
Ag ⁺	silver ion
AgNO ₃	silver nitrate
EtOH	ethanol
EtOAc	ethyl acetate
ACN	acetonitrile
TOL	toluene
EG	ethylene glycol
i-BuOAc	iso-butyl acetate
n-BuOH	n-butanol
DMF	dimethylformamide
DMA	dimethyl amine
PATP	4-aminonitrophenol
DI	de-ionized
UV-Vis	ultraviolet-visible
TEM	transmission electron microscopy
TGA	thermal gravitation analysis
XRD	X-ray diffraction

FT-IR	Fourier-transform infrared spectroscopy
SEM	scanning electron microscope
EDX	energy dispersive X-ray spectrometer
LSPR	localized surface plasmon resonance
SERS	surface-enhanced Raman spectroscopy
CMC	critical micelle concentration
CVD	chemical vapor deposition
nm	nanometer
g	gram
mg	milligram
L	liter
μm	micrometer
mL	milliliter
mM	millimolar
ppm	part per million
$^{\circ}\text{C}$	degree Celsius
min	minute
rpm	revolutions per minute
cps	count per second
cm^{-1}	reciprocal centimeters
wt%	weight-weight percentages
2θ	2 theta
deg, $^{\circ}$	degree
R^2	linearity

CHAPTER 1

INTRODUCTION

Silver nanoparticles (AgNPs) have tremendous applications in several area including catalysis [1], electronic [2], optical sensors [3] and antibacterial agents [4] etc. because of their size- and shape-dependent optical, electrical, electronic and antibacterial properties. Therefore, a number of protocols have been proposed for synthesis and stabilize AgNPs as shown in Table 1.1.

Table 1. 1 Physical, chemical and photochemical methods synthesis and stabilize AgNPs.

Method	Silver precursor	Reducing agent	Stabilizing agent	Size (nm)
Chemical reaction	AgNO ₃	DMF	-	<25
	AgNO ₃	NaBH ₄	lipopeptide biosurfactant	3-28
	AgNO ₃	TSC+SFS	TSC	<50
	AgNO ₃	TSC	-	30-60
	AgNO ₃	Ascorbic acid	DDA	200-650
	AgNO ₃	NaBH ₄	oleylamine	~ 7
	AgNO ₃	paraffin	PVP	10-14
	AgNO ₃	dextrose	-	22 ± 4.7
	AgNO ₃	hydrazine	gluconic acid	2-10
	AgNO ₃	glucose	PVP	40-80
	AgNO ₃	ethylene glycol		5-25

Table 1. 1 (cont.)

Method	Silver precursor	Reducing agent	Stabilizing agent	Size (nm)
Chemical reaction	AgNO ₃	ethylene glycol	PVP	50-115
	AgNO ₃	cathode: Ti , anode: Pt	PVP	~11
	AgNO ₃	m-hydroxy benzaldehyde	SDS	15-260
	AgNO ₃	hydrazine hydrate	AOT	2-5
	AgNO ₃	hydrazine hydrate	AOT	<1.6
Physical synthesis	AgNO ₃	Electrical arc discharge	sodium citrate	14-27
Photochemical reduction	AgNO ₃	Ethylene glycol	PVP	5-10
	AgNO ₃	UV light	-	4-10
	AgNO ₃	CMCTS, UV	CMCTS	2-8

DMF; *N, N'*-dimethylformamide, NaBH₄; sodium borohydride, TSC; tri-sodium citrate, SFS; sodium formaldehyde sulfoxylate, DDA; dodecanoic acid, PVP; polyvinyl pyrrolidone, SDS; sodium dodecyl sulphate, AOT; Bis (2-ethylhexyl) sulfosuccinate, CMCTS; carboxymethylated chitosan.

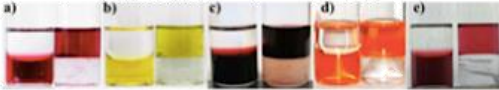
Copyright from Synthesis of silver nanoparticles: chemical, physical and biological methods.

Research in Pharmaceutical Sciences [50].

Due to the metal precursor (AgNO₃), most of those listed protocols were preferably performed in either water or water-miscible solvents [5,6,7]. In these solvents, AgNPs are generally synthesized *via* the chemical reduction of silver ions with a reducing agent and control size and shape by an additional stabilizer [8,9,10]. On the other hand, the synthesis of AgNPs in organic solvents is complicated and should be well-designed. For a widely usage AgNPs in nonpolar organic system, the transferring protocol of AgNPs is an alternative way to transfer AgNPs in water to organic solvents

[11,12,13]. There are several proposed approaches based on transferring process to move AgNPs into organic solvents. Many authors reported transferring AgNPs into an organic phase by hydrophobization of the particle surface using various ligands such as alkylamines [14,15], ionic surfactants [16,17] and amide coupling agents [18] as shown in table 1.2.

Table 1. 2 The phase transfer of AgNPs into organic solvents by using various ligands.

ligands	Researchers	Summary
Alkylamines	X. Wang <i>et. al.</i> ^[14] Pino., P. <i>et. al.</i> ^[15]	AgNPs (<118 nm) were transferred into chloroform by using octadecylamine (ODA). The synthesized AgNPs and AgNPrs were stabilized by PEG and transferred into chloroform by using dodecylamine (DDA).
Ionic surfactants	C., Shen-Hao <i>et. al.</i> ^[16]	The synthesized AgNPs in water were transferred to chloroform by the inducer dimethyldioctadecylammonium chloride (DDAC).
	Bigioni., P., T. <i>et. al.</i> ^[17]	AuNPs were demonstrated to transfer into toluene by using various ionic surfactants.  <small>Phase transfer from water (lower phase) into toluene (upper phase) using both TOAB and C16TAB surfactants, with (a) 13.1 nm citrate-capped Au NPs, (b) 13.5 nm citrate-capped Ag NPs, (c) Na₂S₂O₄-MBA₂ clusters, and (d) 5 nm citrate-capped CdSe quantum dots. (e) TOAB and C16TAB surfactants were used to phase transfer 16.1 nm citrate-capped Au NPs.</small>
amine coupling agent	Kelly., L., T. <i>et. al.</i> ^[18]	AgNPrs were synthesized and modified with 16-mercaptohexadecanoic acid (MHA) and transferred to chloroform through EDC coupling with dicyclohexylamine.

Such phase transfer procedures are very useful as aqueous phase synthesis of AgNPs is relatively simple, inexpensive and more reproducible. Furthermore, the shape and size of AgNPs can be easily controlled using suitable stabilizers. However, there is a few severe limitations of these transferring process as (i) amount of transferring agents should be carefully optimized as they can be possibly from double layers around the particle, (ii) only the particles with small size are possibly transferred and (iii) surface of the particle are dirty with the covered transferring agent molecules.

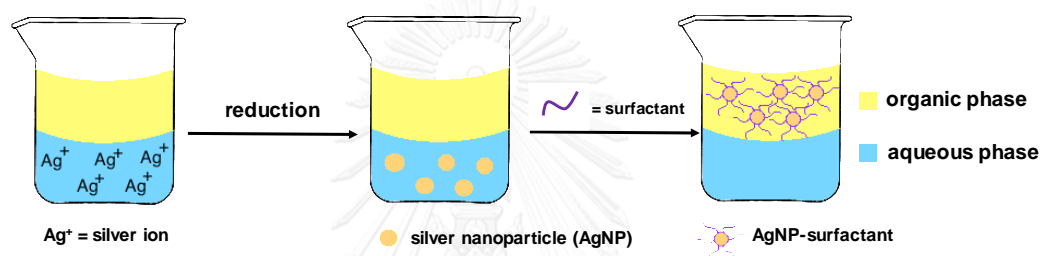


Fig. 1. 1 Phase transfer of AgNPs by using surfactant.

To overcome these limitations, the carrier system has been developed to transfer the AgNPs to organic solvents as shown in fig 1.2. The system uses a carrier material as a transferring agent instead of the surfactant. However, the type of carrier material should be well considered as it should provide the functional groups to stabilize AgNPs, no effect on the properties of AgNPs, inert to any chemical reaction and possibly disperse in both polar and non-polar organic solvents.

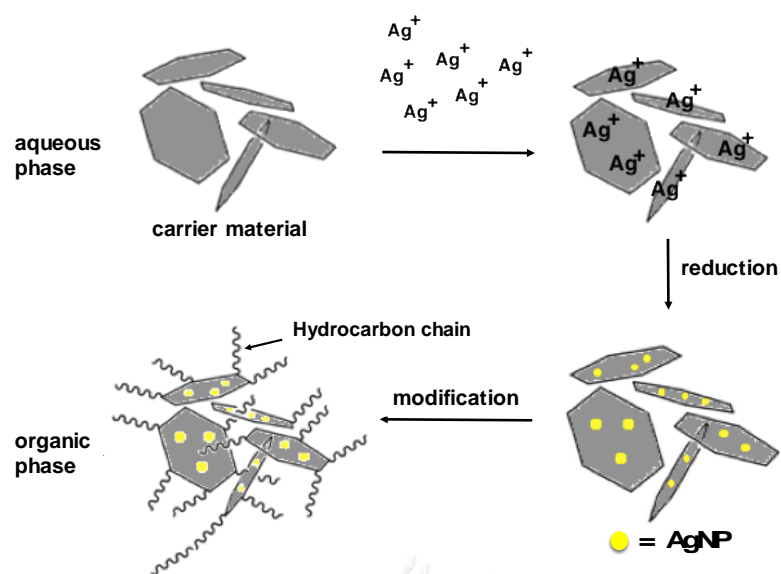


Fig. 1. 2 Phase transfer of AgNPs by using a carrier system.

Graphene is an atomically thin layer of sp^2 -bonded carbon atoms, stacked in a two-dimensional (2D) lattice and has attracted an extraordinary amount of interest due to the thermal, optical, and mechanical properties. Graphene is firstly synthesized from graphite by the mechanical exfoliation which is a laboratory procedure and not possible to synthesize the high-quality of graphene. Many researchers have been reported the protocols to synthesize of isolated graphene monolayer such as chemical vapor deposition (CVD), chemical conversion and reduction of carbon monoxide as shown in fig. 1.3 [59]. Although, those protocols produced the high-quality of graphene monolayer, it might not possible to synthesize with a large scale.

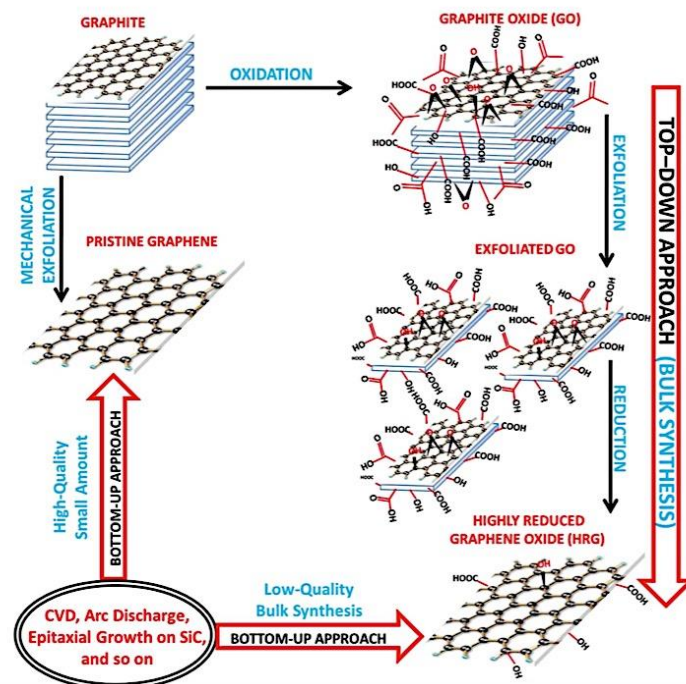


Fig. 1. 3 Schematic illustration of the synthesis of graphene [59].

To overcome this limitation, chemical oxidation of graphite is an alternative option to fabricate a large amount of graphene colloidal solution and easily developed from the industrial production using graphite as an inexpensive raw material. This process can be generated graphene oxide (GO) which is an oxidized graphite. GO have their basal planes contain the oxygen function groups e.g. epoxide, hydroxyl and carbonyl and carboxylic groups at the edges of the GO sheets [19,20]. Because of oxygen rich functional groups, the GO colloids are well-dispersed in polar solvents especially water media. Therefore, the preparation of dispersed GO for applications such as printed flexible electronics, conductive polymers, ceramic coating, water purification and biomedical manufactured using organic solvents as a media might not be a straightforward process due to the stability in those organic solvents is a critical point to be concerned. The dispersibility of the modified GO in various solvents (including organic solvents) has been examined by several research groups. Chung *et.*

al. [21] successfully used the alkylamine-functionalized graphene oxide (FGOs) to uniformly distribute the polystyrene (PS) matrix in chloroform. Khatri *et. al.* [22] reported the preparation of alkylated graphene by the coupling of the carboxylic groups of graphene oxide (GrO) with various alkylamine ($C_n = 8, 12, 18$) for lubrication applications. The long term dispersion stability of the alkylated graphene was observed in different six organic solvents and found that the stability of alkylated graphene in organic solvents was depended on the chain length of alkyl groups. Xie *et. al.* [23] developed the phase transfer method of graphene oxide nanosheets (GONs) from water to non-polar organic solvents by modifying the GONs surface with oleylamine.

The synthesis of graphene composites with precious metal nanoparticles has recently received great interest for the novel optical, electronic, mechanical and catalytic properties of the composites. In case of AgNPs decorated graphene, it is the most promising composite for catalysis [24], electrochemistry [25], SERS materials [26], biosensors [27] and specially for enhancing antibacterial activity [28,29]. The GO/AgNP composite has been discovered as a good resistance material for bacteria growing [30,31,32,33]. Therefore, the composite of GO/AgNP was clinically used in several medical researches. According to a great potential of the composite, the fabrication of GO/AgNP composites received a great interest from several research groups. They mostly focused on the synthesis of the GO/AgNP composites by physical and chemical methods as described in table 1.3.

Table 1. 3 The preparation of GO/AgNP composites.

Years	Researchers	Procedures	Applications
2015	Elimelech, M. <i>et. al.</i> ^[34]	GO-Ag nanocomposite was synthesized by chemical reaction, using NaBH ₄ as a reducing agent at room temperature for 12h and fabricated with PGLA-chitosan nanofiber.	antimicrobial
2013	Chia, C. H. <i>et. al.</i> ^[35]	FGO was used as substrate, reducing agent and stabilizer for AgNP in alkaline medium by simple stirring method.	antibacterial and SERS
2011	Sun, X. <i>et. al.</i> ^[36]	AgNPs/GN was prepared by Microwave-assisted reduction, using DMF as a reducing agent with 750 watt for 2 min.	hydrogen peroxide detector
2010	Ye, M. <i>et. al.</i> ^[37]	Ag-CCG nanocomposite was prepared by chemical reaction, using NaBH ₄ ethylene glycol as reducing agents and heated at 110 °C for 2 hrs.	antibacterial and SERS
2009	Zhang, H. <i>et. al.</i> ^[38]	AgNPs were directly reduced on GO substrate without reducing agent. The solution was heated at 75 °C for 30 min under N ₂ .	-

From the literatures, the GO has emerged as a material that is often used to support and stabilize AgNPs for the preparation of novel nanocomposites for antibacterial [34], SERS substrates [35] and sensor [36]. GO is not only providing strong interaction with the AgNPs but also enhances the properties of AgNPs. According to the electronic charge of AgNP and oxygen rich functional groups on the graphene oxide, the composite of GO/AgNP might be dispersed in the strong polar solvents and water. However, the functional groups on GO nanosheets allows us to modify in order to increase hydrophobicity for transferring them into non-polar solvents. Therefore, GO

might be considered as a good carrier material to transfer the AgNPs to organic media. Until now, no data exists to concern the phase transfer of the GO/AgNP composites in organic solvents. If the transferring protocol of the GO/AgNP composites is successfully developed, this will open up the new applications of the composites in electronics, polymers, coating *etc.*

1.1 The objectives

To developed a simple, non-toxic, cost-effective, quick and environmentally synthesis approach to fabricate graphene oxide based composite with silver nanoparticle (GO/AgNP composites) and the effective protocol to modify them to form stable suspensions which can be well-dispersed in several organic solvents.

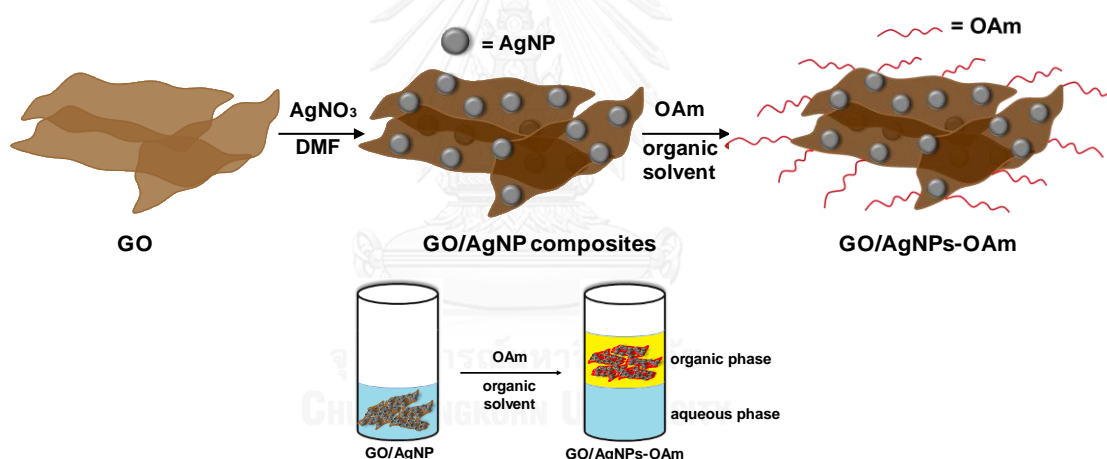


Fig. 1. 4 Schematic illustration of the synthesis and phase transfer process of GO/AgNP composites using OAm as a transferring agent.

1.2 Scopes of this research

1. Synthesized GO/AgNP composites by chemical reaction, using DMF as a reducing agent.
2. Modified GO/AgNP composites by alkyl amine, improving hydrophobic property.
3. Dispersed the modification of GO/AgNP composites in organic solvents.

CHAPTER 2

THEORETICAL BACKGROUND

2.1 Silver nanoparticles (AgNPs)

Silver nanoparticles (AgNPs) have been received the great attraction due to their unique different properties which exhibits the potential applications from bulk materials such as catalysis activity, electrical conductivity, optical properties and antibacterial activity. The synthesized protocol to fabricate AgNPs have been developed by chemical, physical, photochemical and biological approaches. Mostly, the AgNPs was prepared in aqueous solution by chemical reduction methods due to the initial precursors which usually consist of (I) silver salt precursors, (II) reducing agents (*e.g.* sodium borohydride, glucose, ascorbic acid, tri-sodium citrate) and also (III) stabilizers. In the reaction, the silver ions (Ag^+) were reduced by reducing agent and lead to the formation of metal silver (Ag^0) to AgNPs. Then, size and shape of AgNPs will be controlled by stabilizers (*e.g.* starch, polyvinyl pyrrolidone, polyvinyl alcohol).

The optical properties of AgNPs involves the co-ordination of delocalized electron oscillation at the AgNP surface called “Localized surface Plasmon resonance (LSPR)” as shown in fig. 2.1 [39]. LSPR related shape and size of nanoparticles which were also affected the absorbance spectra in UV-Vis technique and corresponds to the appearance color. The changing in solution color was referred the changing in size and shape of nanoparticles. Thus, these properties utilize to a powerful sensor device.

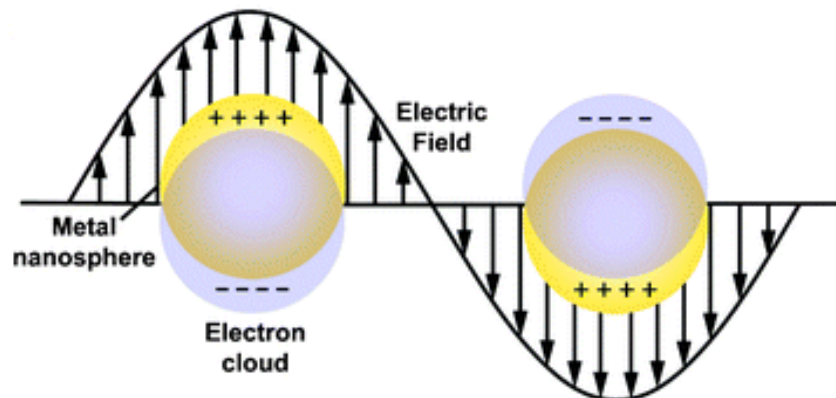


Fig. 2. 1 Localized surface Plasmon resonance of nanoparticles [39].

Anti-bacterial activities were the distinguished properties of AgNPs which had attracted much interests from many researchers. The distribution of silver ions from AgNPs at the cell wall punctured in-side the cell and contributed the condensation with DNA of bacteria as shown in fig. 2.2 [40]. The anti-bacterial mechanism was explained that silver ions reacted thiol groups (-SH) of protein at cell membrane. This interaction caused the dysfunction of transportation between cells and lead to the bacterial cell death. Therefore, AgNPs become the part of important materials for housewares and health care products such as detergents, toothpastes, socks, pillows, bandages, washing machines as well as water purifier.

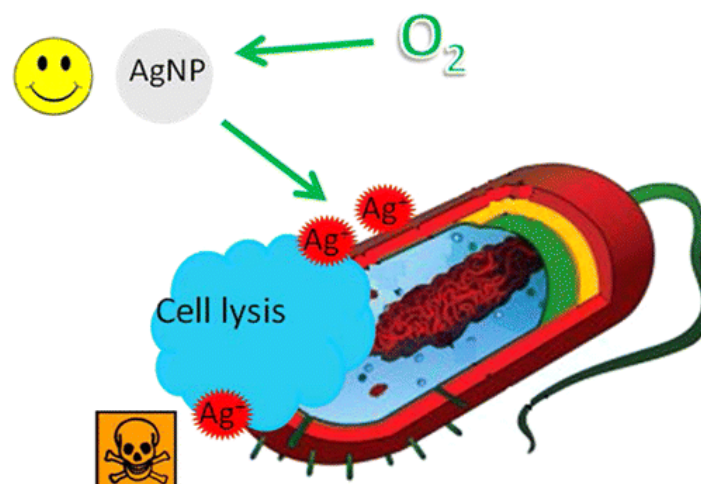


Fig. 2. 2 The anti-bacterial mechanism of AgNPs [40].

2.2 Phase transfer method in metal nanoparticles (MNPs)

Due to the great properties of MNP *e.g.* optical sensor, catalyst and electronic device, many researchers reported the protocol to synthesis MNP in both polar and non-polar solvents. The preparation of MNP in organic solvents is the great challenged for scientist in order to open-up the opportunity in industries fields which mainly used organic solvents to produce many products. Some researchers suggested phase transfer method for transferring MNP into organic solvents which is described in this section [41].

Brust-Schiffing method is easily phase transfer by modifying the MNPs surface with long chain hydrocarbon of thiol compound for improving the hydrophobic property. According to thiol functional group, they do easily bind with the surface of AgNP to generate the micelle structure. This enhance the hydrophobicity of MNPs which be possibly dispersed in organic solvents as shown in fig 2.3 [41].

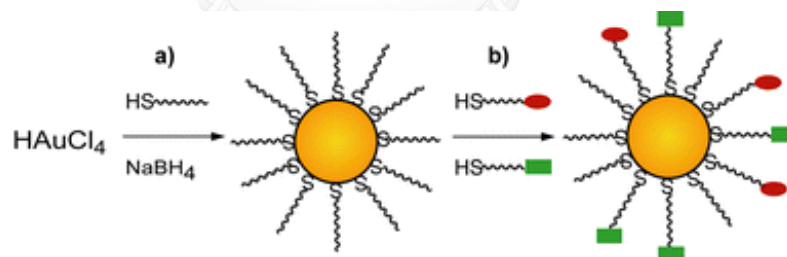


Fig. 2. 3 Schematic of the phase transfer of gold nanoparticles by Brust-Schiffing method [41].

Phase transfer of “naked” nanoparticles is applied the diffusion process. The transferring agent (*e.g.* hydrophobic compounds) in organic phase are immediately reacted with the generated MNPs in water phase. According to hydrophobicity of the MNPs after interacting with a transferring agent, this will rip the MNPs into organic phase as shown in fig 2.4 [41].

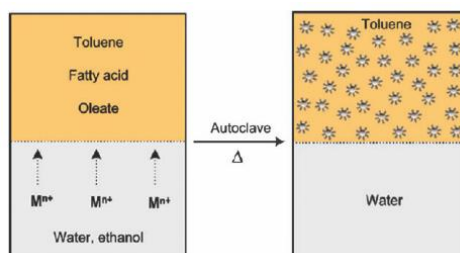


Fig. 2. 4 Schematic of the phase transfer of MNPs by “naked” nanoparticles method [41].

Phase transfer with ligand exchange is the method which involves the exchange process of the capping agents on MNPs in aqueous with another capping agent in organic phase. The MNPs were synthesized in a polar solvent with capping agent while in non-polar solvent had another type of capping agent which trend to have stronger interaction with the surface of MNPs. Therefore, the exchange process will be occurred and transfer MNPs into organic solvents as shown in fig. 2.5 [41].

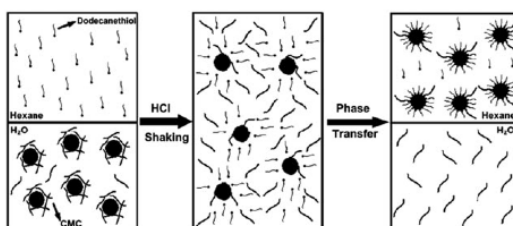


Fig. 2. 5 Schematic of the transferring of MNPs into hexane by ligand exchange method [41].

Phase transfer via electrostatic interaction is the alternative method using the interaction between the transfer agents and MNP surface. For example, in fig. 2.6 [41] showed the arrangement of acid (negative charge) around dendrimers (positive charge) which were assembly on MNPs and transfer MNPs to toluene. As the acid-base interaction, Dendrimers could be shift its form from micelles to inverted micelle.

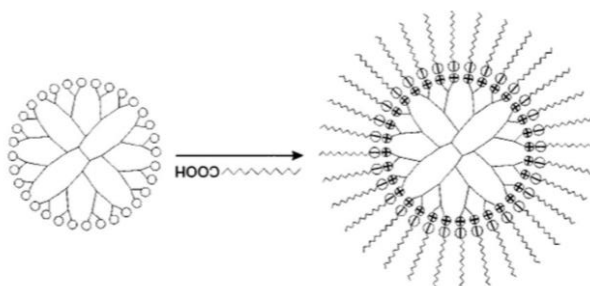


Fig. 2. 6 Schematic of the transferring of MNPs into hexane by electrostatic interaction [41].

From the discussed methods, many researchers interested to transfer MNP into organic solvents. However, the phase transfer methods using capping agents should be well-designed as they are able to be achieved when only critical micelle concentration (CMC) of the capping agent is performed. CMC is the lowest concentration of surfactant that form as micelle for increasing the hydrophobic property of MNP. CMC might be related to size and shape of MNPs in the system. Therefore, if MNPs were synthesized using different conditions, the CMC need to be re-optimized. It can be seen that this transferring process is expensive, low productive and only the small particles could be successfully transferred into organic solvent. Moreover, the modification on MNP surface by capping agent on MNP surface might decrease the potential properties of MNPs.

2.3 Graphene oxide (GO)

Graphene oxide (GO) had a single layered structure similar to graphite oxide as shown in fig. 2.7. There were many authors reported the procedures for preparing GO. Recently, the most common method was the modified Hummers which could be carried out in the oxidation and post-treatment [42]. Briefly, graphite powder was treated by sodium nitrate (NaNO_3) and sulfuric acid (H_2SO_4). The graphite suspension was oxidized by potassium permanganate (KMnO_4) for 12 hours. After that, the suspension was further treated by hydrogen peroxide (H_2O_2). Hydrochloric acid (HCl) and DI water were used to wash the product and purified by dialysis treatment. Finally, graphite oxide powder was obtained after drying by thermal treatment. The single layered GO sheet was produced by simple sonication of the dispersion graphite oxide powder in water. Fig 2.7 represents the schematic drawing of the synthesise process of GO from graphite.

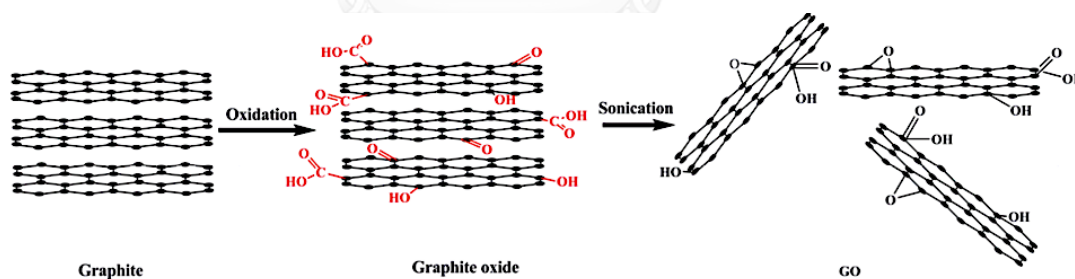
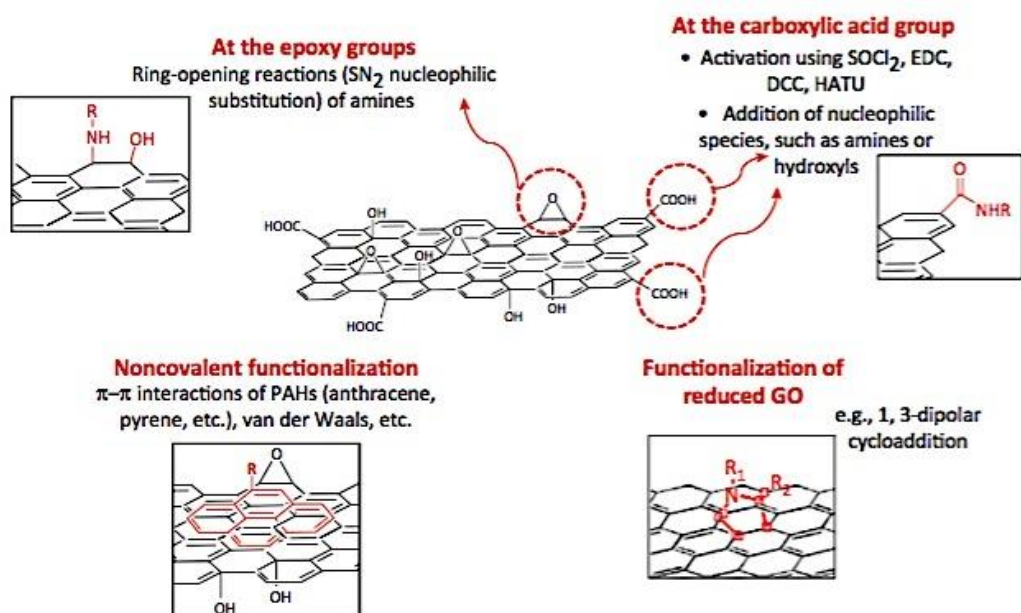


Fig. 2. 7 Structures of graphite, graphite oxide and graphene oxide [19].

Due to the amount of oxygen functional groups from oxidation reaction, the GO structure had enriched with oxygen functional groups; epoxy, hydroxyl at the basal plane and carboxylic acid at the edge. Thus, GO was highly dispersed in water and polar solvents. Moreover, the GO could be easily modified surface for desire application. The chemical functionalization of GO included four reactions [43].

- (I) Nucleophile addition at the carboxylic acid groups by amine or hydroxyl.
- (II) S_N2 nucleophilic substitution by opening the ring of epoxy groups.
- (III) Van der Waals interaction with surfactant and polymer or $\pi-\pi$ interaction with polyaromatic.
- (IV) Cycloaddition and diazonium reaction.



CHULALONGKORN UNIVERSITY

Fig. 2. 8 The functionalized reactions with graphene oxide [43].

2.4 Phase transfer of GO into organic solvents

The preparation of dispersed GO for applications such as conductive polymers, ceramic coating, biomedical and lubricant manufactured using organic solvents as a media might not a straightforward process because of the polarity from oxygen functional groups on GO. Therefore, the modification of GO is required in order to be well-dispersed in organic solvents as shown in fig 2.9.

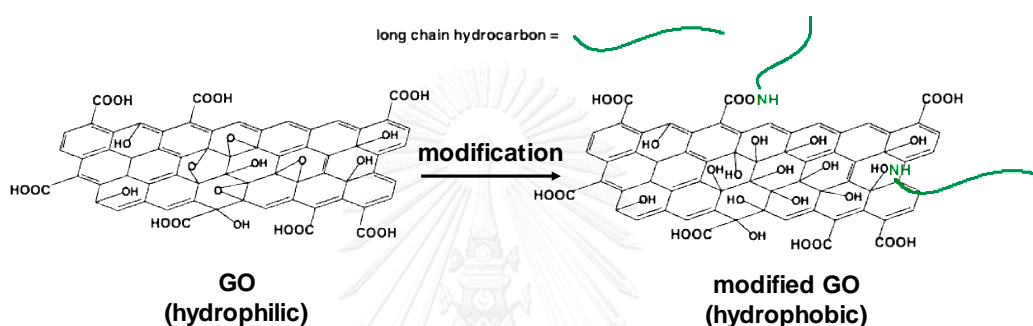


Fig. 2. 9 the modification of GO by various transfer agents.

The transfer agents modify GO at carboxylic groups such as alkylamine; octylamine, dodecylamine, hexadecylamine, oleylamine. While the modification of p-phenylenediamine (PPDA) [44] which is an aromatic diamine will react with GO at epoxy groups. Moreover, organic/inorganic constituents are also used as transfer agent e.g. polyhedral oligomeric silsesquioxane (POSS) [45]. The advantages of modified GO in organic solvents could be concluded as:

- Highly thermal stability composite
- Highly modulus materials
- Additive filler in lubricant industry
- Ceramic reinforced

Thus, the modified GO could be dispersed in organic solvents which is the new material for opening the opportunities in industrial applications.

2.5 The metal on graphene/GO surface

Furthermore, the synthesis of graphene composites with precious metal nanoparticles (MNPs) has recently received great interest due to the unique properties of MNPs which enhanced the potential application of materials based-on graphene composite. According to the composite of graphene with MNP gained the great interest from many research groups, the interaction of MNP on graphene/GO surface was still discussed. The existence of the functional groups on GO surface had the negative charge which occurred the nucleation of the positive charge of metal ions and allowed the formation of MNP on the GO surface [46].

Shin., S., H. *et al* [47] investigated the effect of graphene layer on metal-graphene interaction by surface enhanced Raman scattering (SERS) technique. The enhancement of SERS factors had a result from the deposition of metal on the different graphene layer. Metallic Ag deposited on the single-layer graphene, showing the largest enhancement factor due to the strong interaction between them while the deposition of Ag on bi- and tri-layer graphene were assumed Van der Waals interaction.

Chen., J. *et al* [48] succeeded to synthesis the decoration of aerosol Ag nanocrystals on GO sheets by electrostatic force directed assembly technique. The interaction of Ag nanocrystals on GO sheets was studied by annealing process. After annealing, the low migration of Ag nanocrystals suggested the low activation energy that mean the deposition of Ag nanocrystals on GO surface through Van der Waals interaction.

Biswas., K. *et al* [49] investigated the nature of electronic interaction of metal (Ag, Au) and alloy nanoparticles (AuAg NPs) on graphene nanosheet by Raman spectroscopy. The existence of Ag, Au and AuAg NPs led to red-shift in D and G band in Raman signal which indicated the strong electronic interaction between them.

CHAPTER 3

EXPERIMENTS

3.1 Chemicals and Materials

- Silver nitrate (AgNO_3) (Aencore chemical PTY. LTD)
- 2 mg/mL of Graphene oxide nanocolloids (NGO) (Sigma-Aldirch Co. LLC.)
- Oleylamine (OAm, $\text{C}_{18}\text{H}_{35}\text{NH}_2$) (Sigma-Aldirch Co. LLC.)
- Ethanol (EtOH , $\text{C}_2\text{H}_6\text{O}$) (Merck Sharp & Dohme Corp.)
- Ethyl acetate (EtOAc , $\text{C}_4\text{H}_8\text{O}_2$) (Merck Sharp & Dohme Corp.)
- Acetonitrile (ACN , CH_3CN) (Merck Sharp & Dohme Corp.)
- Dimethylformamide (DMF , $\text{C}_6\text{H}_8\text{O}$) (Carlo Erba reagent S.A.S)
- Toluene (TOL , C_7H_8) (Carlo Erba reagent S.A.S)
- Ethylene glycol (EG , $\text{C}_2\text{H}_6\text{O}_2$) (Carlo Erba reagent S.A.S)
- Iso-Butyl acetate (i-BuOAc , $\text{C}_6\text{H}_{12}\text{O}_2$) (B.D.H Middle East LLC.)
- n-butanol (n-BuOH , $\text{C}_4\text{H}_{10}\text{O}$) (RCI Labscan LTD.)

All reagents and solvents were in analytical grade and were used without further purifications. All glassware and magnetic bars were cleaned with detergent and followed by deionized (DI) water.

3.2 Instruments

- Transmission electron microscopy, Hitachi Model: H-7650
- Thermal gravitation analysis, Perkin Elmer Model: pyris 1TGA
- UV-visible spectroscopy, Thermo Fisher Scientific Model: G10S
- X-ray diffractometer, Rigaku Model: D/MAX-2200
- Fourier-transform infrared spectra, Nicolet 6700
- Raman microscope, Thermo scientific DXR with 780 nm as excitation laser.
- Scanning electron microscope, JEOL JSM-6510
- Built-in energy dispersive X-ray spectrometer, JEOL JSM-6510
- Ultrasonic bath, Elmasonic Model: P30H
- Centrifuge, Hettich Model: EBA 200

3.3 The synthesis of graphene oxide-silver nanoparticle (GO/AgNP) composites

Firstly, the synthesized process of AgNPs by using DMF as a reducing agent was preliminary investigated [53]. To determine the reduction time which Ag^+ were completely reduced to Ag^0 , the LSPR band of the generated AgNPs was monitored at 0 min, 30 min, 1 hour, 2 hours and 3 hours by UV-Vis spectroscopy. After determining the appropriate reduction time, the graphene oxide-silver nanoparticle composites (GO/AgNP) were synthesized as follows.

The stock solution of 1,500 ppm AgNO_3 was prepared by dissolving 0.0778 g of AgNO_3 in 50 mL of DI water. 200 ppm of GO suspension was prepared by mixing 2.5 mL of the 2 mg/mL of GO suspension in 22.5 mL of DI water. The synthesis of the GO/AgNP composites was performed by mixing 25 mL of the prepared 200 ppm GO

with 25 mL of the stock solution of AgNO_3 and then immediately poured in 100 mL of DMF. The mixed solution was stirred and heated in sand bath with controlled temperature at 130-150 °C for 2 hours. After 2 hours, the reaction was incubated under ambient conditions until it cooled down to the room temperature. The solution was then centrifuged at 5,000 rpm for 20 min to separate the GO/AgNP suspensions from the solution. The suspension of GO/AgNPs were washed by DI water for several times in order to remove the excess silver ions (Ag^+) and DMF. Then, the GO/AgNP composites were dried at 60 °C for 3 hours. The existence of AgNPs on GO sheets were characterized by UV-Vis spectroscopy, transmission electron microscopy, Raman spectroscopy, X-ray diffraction, scanning electron microscope-energy dispersive X-ray spectroscopy and thermal gravitation analysis. The schematic process is shown in fig 3.1.

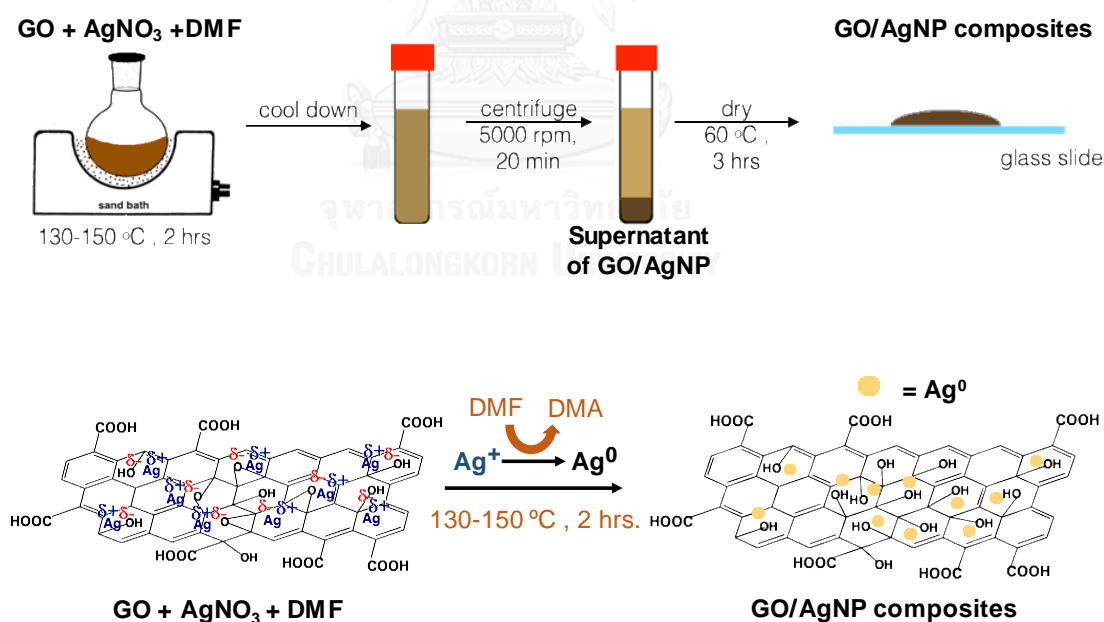


Fig. 3. 1 Schematic drawing of the preparation of GO/AgNP composites by using DMF as a reducing agent (* DMA: dimethylamine).

3.4 The optimization amount of OAm for transferring GO to organic solvents

The turbidity caused by the dispersion of GO suspension was preliminary investigated. The 2 mg/mL GO suspension was diluted at 10, 20, 25, 30, 40 and 50 ppm by DI water and the was detected by UV-Vis spectroscopy, respectively. The calibration curves were generated by plotting the absorbance at 240, 300, 360, 420, 450, 550 and 650 nm against the concentrations of the diluted GO solution. The regression equation with the linearity (R^2) values was calculated for each curve. If the R^2 values closely to 1 was obtained from all curves, this represents that the turbidity is linearly related to the concentration of the dispersed GO suspension. The obtained regression equation was used to determine the amount of the GO suspension in other media *e.g.* organic solvents. This determined amount will be further used to calculate the dispersive efficiency discussed in chapter 4 section 4.2.

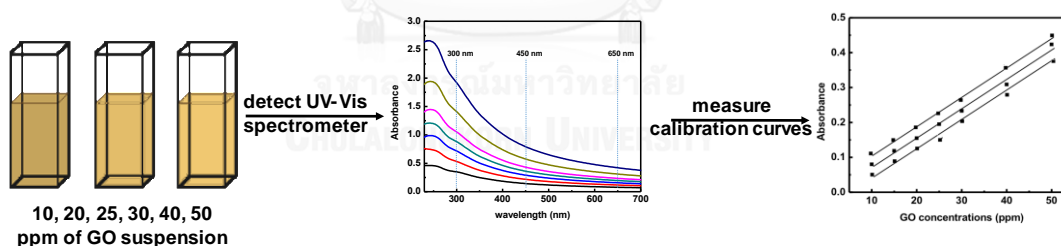


Fig. 3. 2 Schematic illustration showing the measurement of calibration curves.

Due to the abundant of oxygen-functional groups on GO sheets, GO is hardly dispersed in any organic solvents. Oleylamine (OAm) is the long chain hydrocarbon with amine group used as transferring agent for improving hydrophobic property of GO sheets. The amount of OAm for dispersing GO depends on the properties of each organic solvent (such as polarity, surface tension *etc.*). In this experiment, the

appropriate amount of OAm required to transfer the GO suspension for highly dispersed in organic solvents (e.g. toluene, n-butanol, iso-butyl acetate, ethyl acetate, acetonitrile, ethylene glycol) was determined. Firstly, 200 ppm of GO was dried at 50 °C for 12 hours. Then, the OAm solution was directly added to the dried GO colloids with the weight ratios (GO:OAm) at 1:10, 1:50, 1:100, 1:500 and 1:1000, respectively. The GO-OAm mixtures were sonicated for 2 min. until the interaction between OAm and oxygen functional groups on GO colloid was generated. To investigate the dispersion efficiency of the GO-OAm, the 5 mL of those organic solvents were immediately added to prepare the GO-OAm colloids. The mixed solution continued sonication for 1 hour and detected by UV-Vis spectroscopy for measuring the dispersion efficiency of the GO-OAm in the organic solvents.

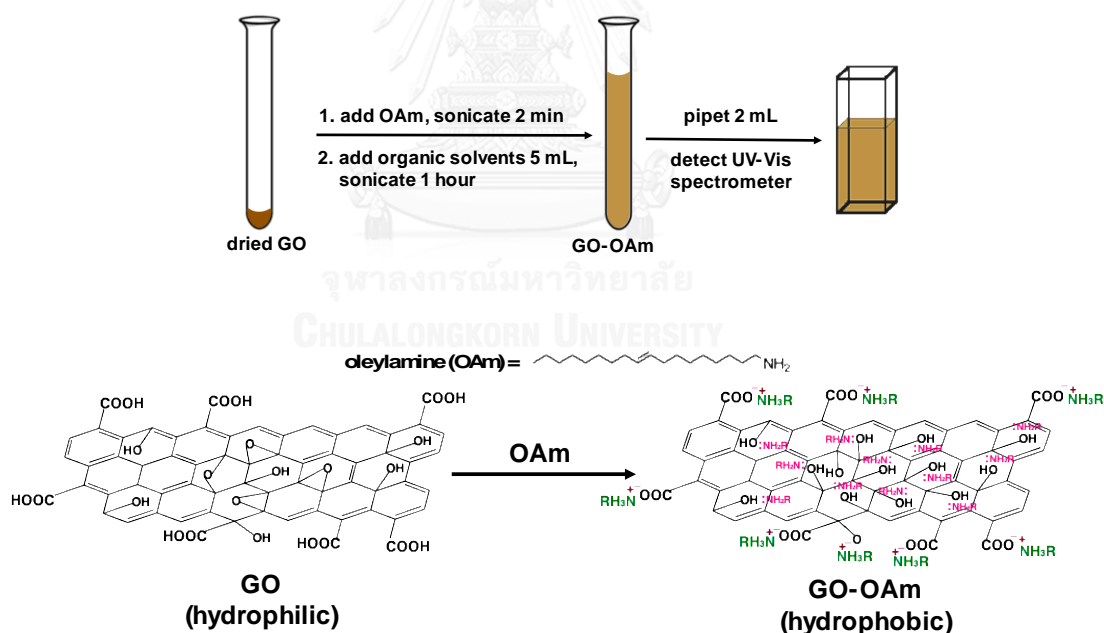


Fig. 3. 3 Schematic illustration of the modification of GO by using OAm for increasing hydrophobicity.

3.5 The GO/AgNPs-OAm composite in organic solvents

After obtaining the optimized amount of OAm for each organic solvent, the appropriate amount of OAm was added to 2 mg of the GO/AgNP composites. The mixture was sonicated by bath sonication for 2 min to generate GO/AgNPs-OAm. To examine the dispersion behavior, the GO/AgNPs-OAm was dispersed in 5 mL of organic solvents; TOL, n-BuOH, i-BuOAc, EtOAc, ACN and EG with bath sonication for 1 hour. The GO/AgNPs-OAm was well suspended in organic solvents affording the formation of a uniform dispersed gray colloid. The persistence of AgNPs on the GO-OAm in organic solvents was observed through the sonication for 30 min and centrifuged 2000 rpm for 10 min to collect the supernatant which was detected by UV-Vis spectroscopy. The stability of the dispersed GO/AgNPs-OAm in the organic solvents were also examined from 0-24 hours. by capturing the images and detected by UV-Vis spectroscopy.

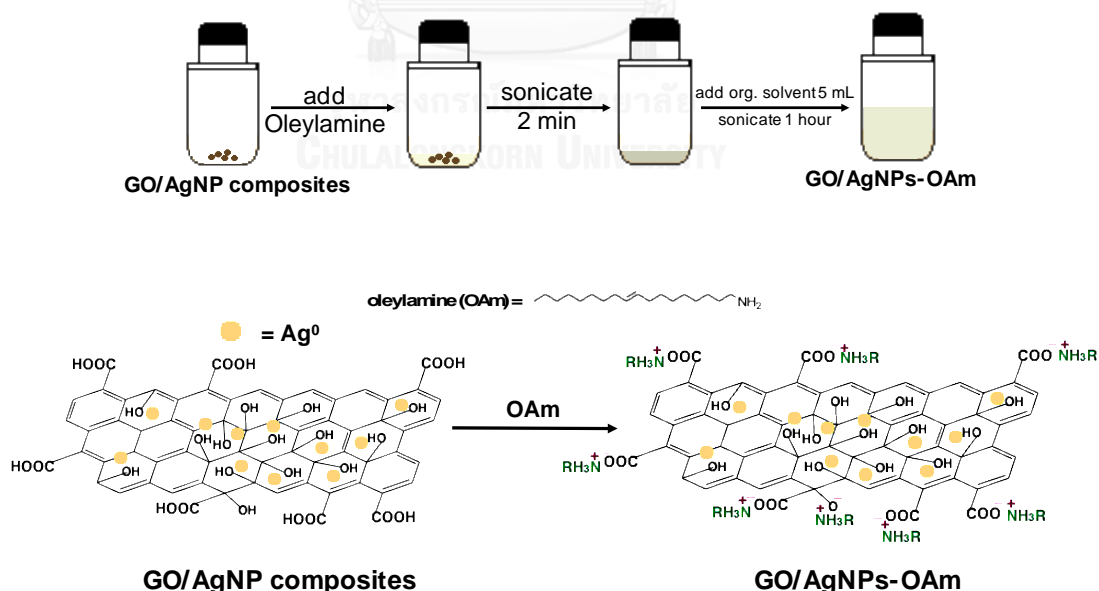


Fig. 3. 4 Schematic illustration of the preparation of the GO/AgNPs-OAm dispersed in organic solvents.

3.6 Characterization

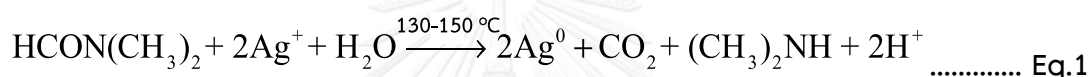
The morphology and decomposition profiles of GO and GO/AgNP composites were examined by transmission electron microscopy (Hitachi Model: H-7650) and thermal gravitation analysis (Perkin Elmer Model: pyris 1TGA) with heating rate 20 °C/min and temperature 60-700 °C, respectively. The formation of AgNPs on GO surface was characterized by UV-visible spectroscopy (Thermo Fisher Scientific Model: G10S) and X-ray diffraction patterns were collected by an X-ray diffractometer (Rigaku D/MAX-2200) with a scanning rate of 0.02 deg/min, using Cu Ka irradiation (0.154 nm, 40kV, 30 mA). The functional groups of GO, GO-OAm, GO/AgNP composite and GO/AgNPs-OAm was characterized by Fourier-transform infrared spectra (Nicolet 6700). The elemental composition analysis of the material was investigated using a built-in energy dispersive X-ray spectrometer (JEOL JSM-6510).

CHAPTER 4

RESULTS AND DISCUSSION

4.1 The synthesis of GO/AgNP composites

AgNPs were synthesized by using DMF as a reducing agent. The formation of AgNPs was occurred along with the decomposition of DMF to carbon dioxide and dimethylamine ((CH₃)₂NH) as shown below [53]. The optimized reaction time was investigated after adding the mixed solution of GO and AgNO₃ into DMF which were heated in sand bath at 130-150 °C.



The color of the GO/AgNP solution at 0 min was light brown. The solution color begins to be changed to dark brown after 30 min. The black sediment was initially observed on the surface of the cuvette (see an inset of fig. 4.1) when the reaction was prolonged for 3 hours. The formation of AgNPs against the reaction time was carried out using UV-Vis spectroscopy as shown in fig. 4.1.

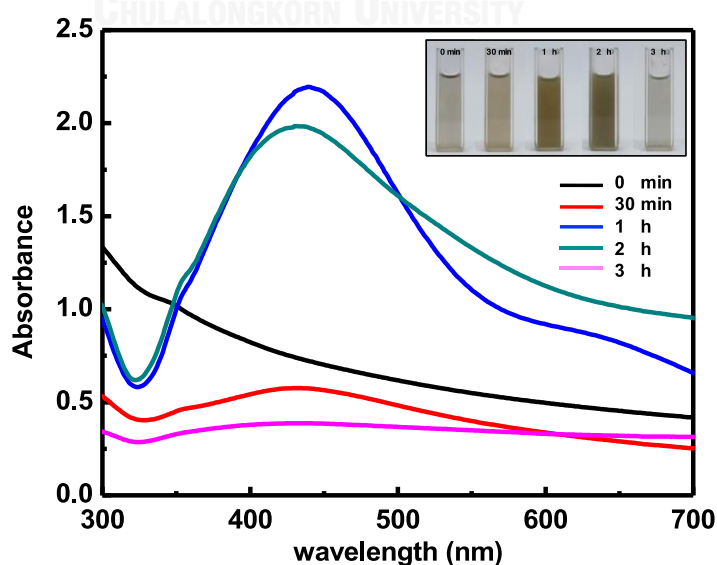


Fig. 4. 1 UV-Vis spectra of the synthesized GO/AgNP composites at the different reaction times.

The appearance of characteristic localized surface Plasmon resonance band (LSPR) at ~430 nm indicated the formation of AgNPs generated since the reaction was incubated for 1 hour. However, there was no visibly observation of the LSPR band after 3 hours. without a sufficient stabilizer, this observation might relate to the indications of sedimentation, aggregation and agglomeration of the generated AgNPs. Although the fact that the peak of the reaction time at 1 hour. shows the highest absorbance, but the free silver ions might remain in the reaction at that time. In order to ensure that the remaining silver ions (Ag^+) was completely reduced to Ag^0 (no free silver ions in the reaction), the reaction time of 2 hours. was chosen to prepare the AgNPs for the GO/AgNP composites.

To fabricate the GO/AgNP composites, the GO nanosheets with the AgNPs synthesized using DMF were performed. The prepared GO/AgNP composites were purified by centrifugation and followed by washing with DI water for several times. The UV-Vis spectra of the GO/AgNP composites compared with the original GO suspensions is shown in fig. 4.2. The appearance of characteristic LSPR band at ~430 nm indicated the formation of AgNPs on the GO nanosheets while only baseline shift without any characteristic peak was observed from the GO suspensions. This indicates that the synthesise of AgNPs on the GO nanosheets using DMF as a reducing agent was successfully developed. Moreover, the stability of the deposited AgNPs on the GO nanosheets was also examined. The suspension of the GO/AgNP composites were strongly sonicated for 30 min and then were centrifuged using 2000 rpm for 10 min. Due to this centrifuge power, only the suspension of the GO/AgNP composites will be precipitated, while individual AgNPs still be dispersed in supernatant as shown in fig 4.2A. UV-Vis spectrum of the supernatant shows only baseline shift without any characteristic LSPR peaks of AgNPs. This suggests that the generated AgNPs were strongly attached on GO nanosheets and were not detached from GO nanosheets by sonication process.

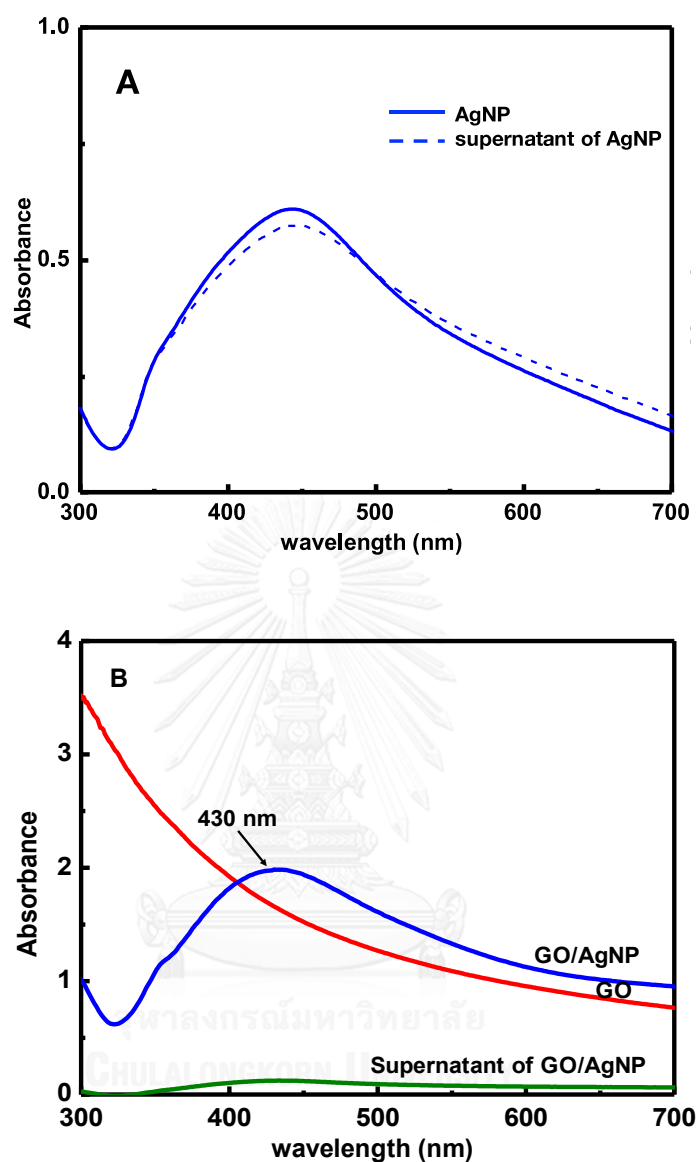


Fig. 4. 2 (A) UV-Vis spectra of the AgNP (solid line) by using DMF as reducing agent and supernatant of AgNP solution after centrifuging at 2000 rpm for 10 min (dot line). (B) UV-Vis spectra of GO/AgNP composites (blue line), the original GO suspension (red line) and the supernatant of GO/AgNP composites after centrifuge 2,000 rpm for 10 min (green line).

The level of deposition of AgNPs on GO nanosheets was assessed by the thermal gravimetric analysis (TGA) under N_2 environment. The weight ratio of AgNPs on GO nanosheets was evaluated by TGA thermograms of weight loss as a function of

temperature. The representative TGA analysis curves of the GO suspension and GO/AgNP composites are shown in fig. 4.3. TGA thermogram of GO suspension shows two weight loss profiles at 150-250 °C and 480-500 °C. The weight loss profile (~20%) at 150-250 °C relates to the evaporation of the absorbed water molecules on GO surface while weight loss (~40%) at 480-500 °C was from the decomposition of oxygen-containing functional groups [54]. However, TGA thermogram of GO/AgNP composites shows higher thermal stability. Only weight loss profile at 150-250 °C due to evaporated water was observed with only 5 % weight loss. This smaller relative weight loss percentage suggests that there are enormous existed AgNPs on GO nanosheets. There is no weight loss profile at 500 °C which might relate to the strong interaction between oxygen functional groups and the generated AgNPs. Correspondingly, the anchoring amount of AgNPs on GO nanosheets was approximately 80 wt%.

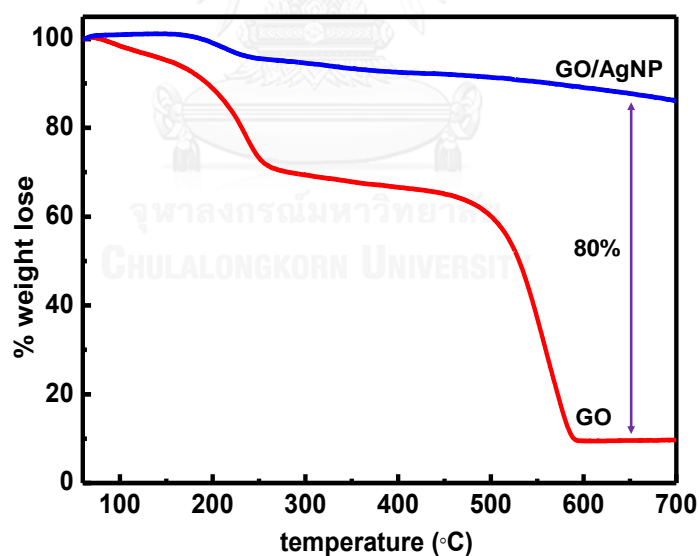


Fig. 4. 3 TGA thermograms of the original GO suspension (red line) and the GO/AgNP composites (blue line).

The formation of AgNPs on GO nanosheets was further confirmed by Raman spectroscopy. The potential applications of AgNPs was used as a surface-enhanced Raman (SERS) substrate to enhance Raman intensity of the chemical compounds. In this case, 4-aminonitrophenol (PATP) was used as a chemical agent to examine the existence of the AgNPs as a thiol functional group of PATP strongly binds with AgNP surface resulting the observation of the strong Raman signals [55]. Fig. 4.4 shows the Raman spectra of the 30 mM of PATP on the GO and the GO/AgNPs. The peaks at $\sim 1350\text{ cm}^{-1}$ and 1580 cm^{-1} were found in GO and GO/AgNP which represented the characteristic of D band and G band of the graphene oxide, respectively [42]. The peak at 1075 cm^{-1} corresponding to C-S stretching of PATP [55] was found using GO/AgNP as substrate, while the peak was not observed from using the GO. This enhancement phenomenon of the PATP indicate the presence of AgNPs on the GO/AgNP composites.

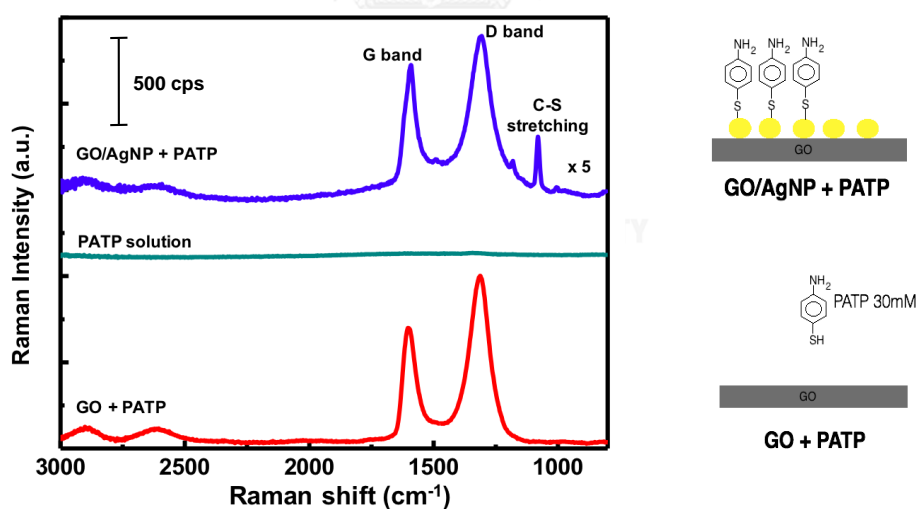


Fig. 4. 4 Raman spectra of PATP 30mM using the GO and the GO/AgNP composites as SERS substrate.

Energy-dispersive X-ray spectroscopy (EDX) was used for determining the elemental compositions on the GO/AgNP composites. The samples were prepared by

dispersing the composite of GO/AgNP in water and dropping on gold plate. Fig. 4.5A showed the EDX spectra and element maps of the GO/AgNP composites in the total detection area. The table results revealed the element compositions including carbon (C), silver (Ag), gold (Au). The most abundant of C atom was determining as the major element of the GO. The amount of Ag atom reported with 17.29 % atoms while the amount of Au was too small portion at this chosen area. From the element mapping, the amount of elements was represented by the color shading on the maps. The color shading of pink and blue refer to the higher amount of element and the trace amount of the detected element, respectively. The mapping of Ag and C element shows the large position on the surface of the synthesized GO/AgNP composites. These results suggested that Ag atom was certainly attached and uniformly distributed on the GO surface. Moreover, the a few selective areas were inspected. At the point 1 and point 2 (see in fig. 4.5B) showed the percents of Ag atom with 19.87 and 20.95, respectively. As the results proved the composite of GO which was consist of Ag metal.

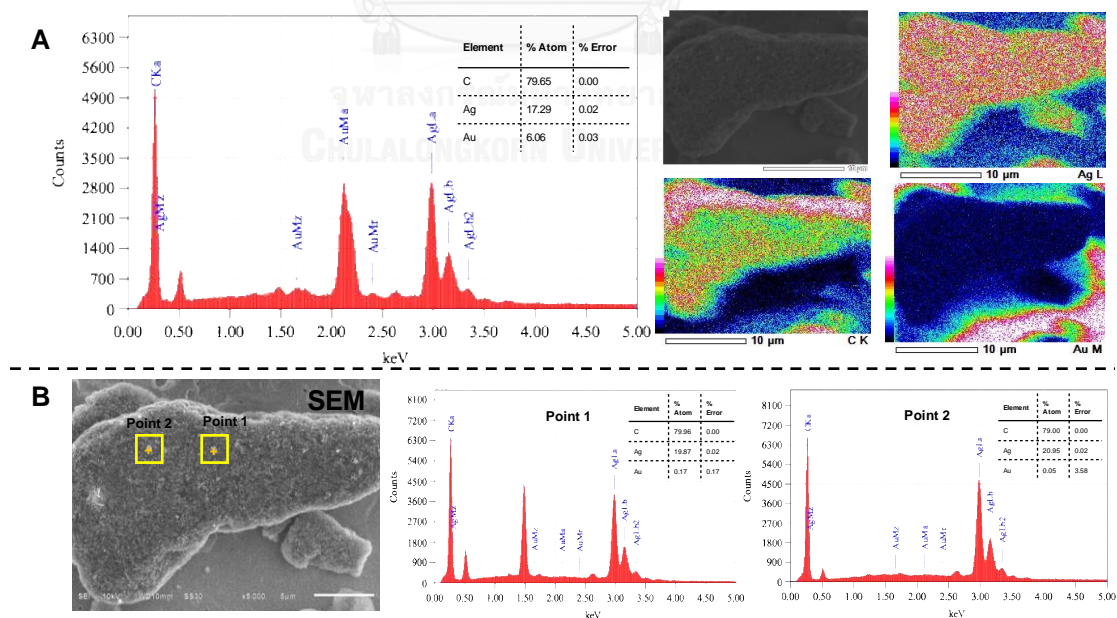


Fig. 4. 5 (A) EDX spectrum and elemental maps of GO/AgNP composites. (B) the EDX analysis on a few selected areas of the GO/AgNP composites to determine the element compositions.

X-ray diffraction (XRD) technique was used to determine the purity of AgNPs deposited on the GO sheets. XRD pattern of the GO/AgNP composites was shown in fig. 4.6. The peaks at 2θ values of 38.2° , 44.3° , 64.5° and 77.5° are assigned to the (111), (200), (220) and (311), respectively corresponding to crystalline planes of the face centered cubic (fcc) of Ag metal (JCPDS no. 65-2871). The high intense diffraction peak observed at 38.2° , corresponding to the crystalline Ag, represent that the nanoparticles are composed of pure crystalline Ag.

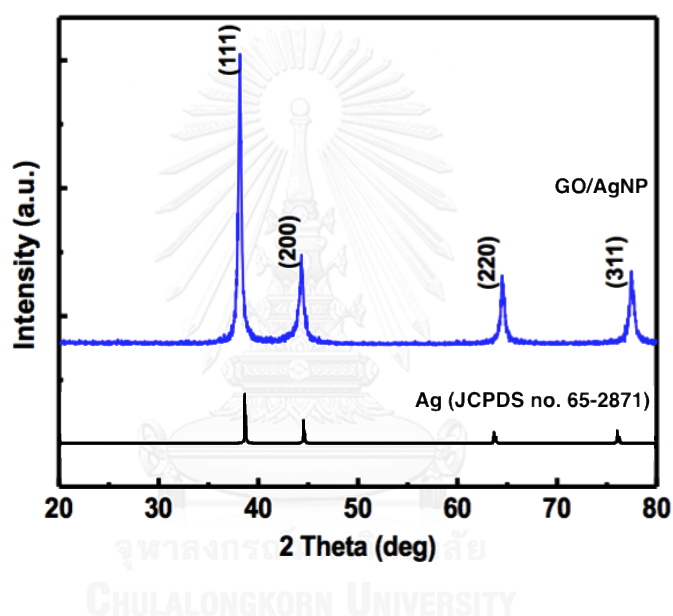


Fig. 4. 6 XRD patterns of Ag metal standard (black line) and the GO/AgNP composites (blue line).

The morphology of GO and GO/AgNP composites were examined by transmittance electron microscopy (TEM) technique. The GO suspension and GO/Ag composites were diluted in DI water and dropped on copper grids for sample preparation. Fig. 4.7A showed the TEM images of a single layer GO nanosheets which was in form of flat layer with large lateral size ($> 10 \mu\text{m}$). On the other hand, the AgNPs represented by dark spots were homogeneously assembled on the micron scale GO which were clearly noticed from TEM images of GO/AgNP composites as shown in fig

4.7B. The strong corrugation of GO surface after deposition of AgNPs with a serious aggregation was observed. This phenomenon evidently induces the aggregation of silver particles. In addition, fig. 4.7C expresses the histogram of the size distribution from TEM images which indicated the average size of AgNPs is approximately 45 nm counted from 100 individual particles with a spherical geometry.

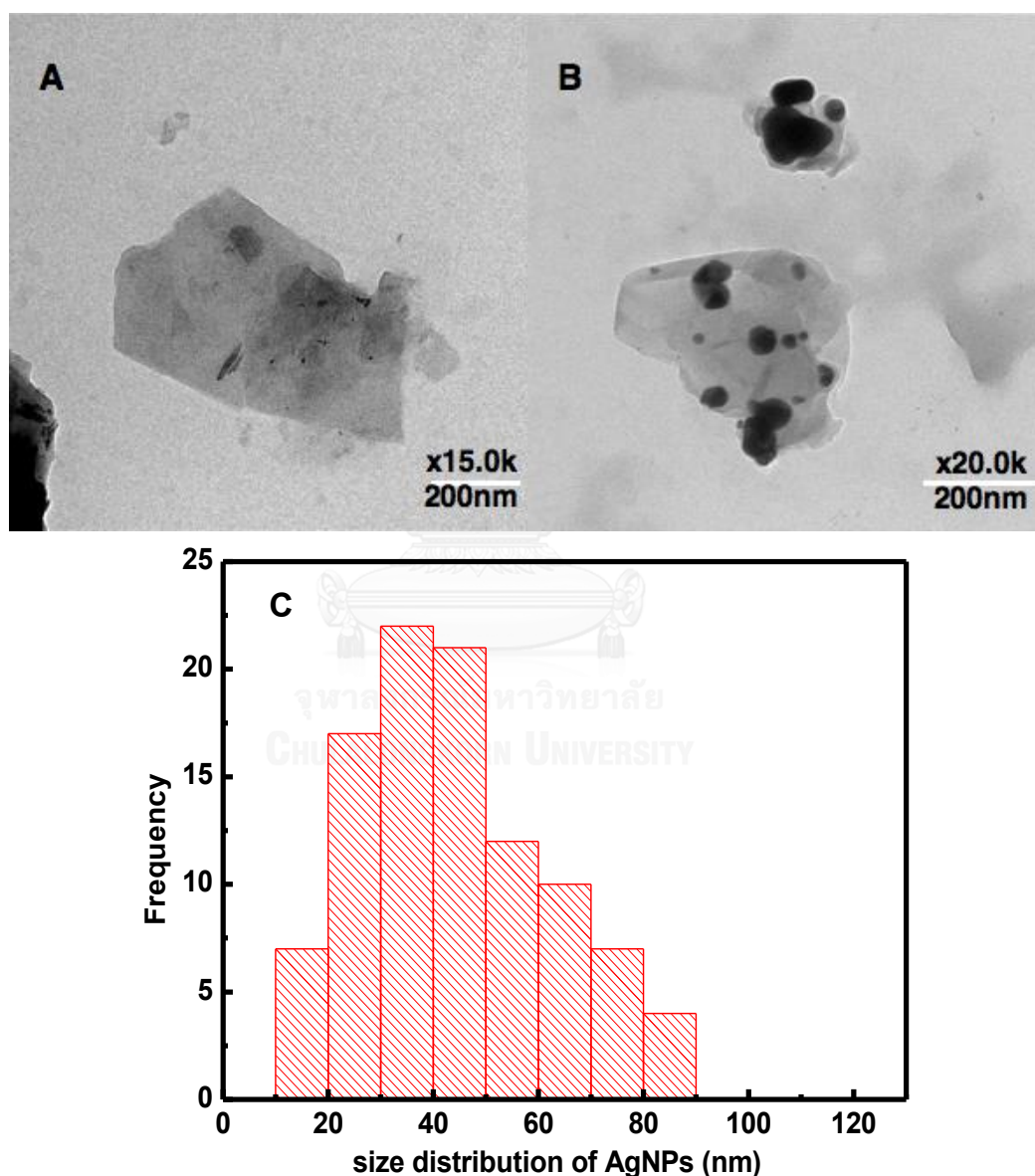


Fig. 4. 7 TEM images of (A) the original GO suspension and (B) the GO/AgNP composites. (C) Histogram of the size distribution of AgNPs on GO nanosheets.

solvents, improving the hydrophobic property of GO surface might be required. The dispersion of GO suspension in aqueous solution was preliminary investigated. Fig. 4.9 showed the UV-Vis spectra of various concentrations (10 ppm to 50 ppm) of the GO suspension in aqueous solvent. It can be seen there was no specific band on UV-visible spectra of GO suspension but only the background intensity was linearly related to the concentration of GO. The higher concentration of GO, the higher background intensity appears.

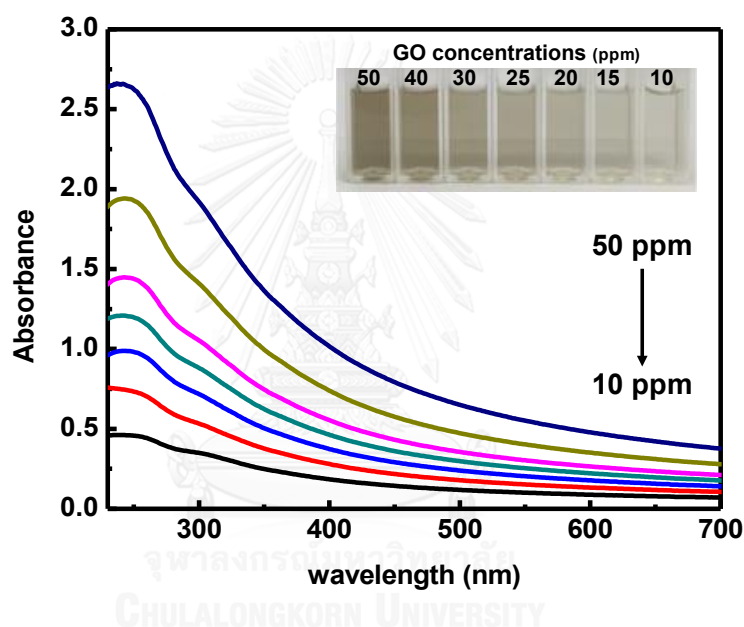


Fig. 4. 9 UV-Vis spectra of the GO suspension at various concentrations (10-50 ppm). The inset image represents the solution containing the dispersed GO suspensions.

To reveal the uniformity of the dispersed GO suspension, the calibration curves between the absorbance collected at 240, 300, 360, 420, 450, 550 and 650 nm and the concentrations of GO suspension (10-50 ppm) were generated as shown in fig 4.10. The regression equations and linearity (R^2) values were calculated in table 4.1. From the results, the R^2 values from the chosen wavelengths are higher than 0.99 and they are insignificantly different. The R^2 closely to 1 was obtained from all curves, this

suggests that the appeared turbidity is linearly related to the concentration of the dispersed GO suspension. The phenomenon reveals that the GO suspension were well dispersed with uniformly distributed across the solution.

To avoid the characterized peak of AgNPs (~430 nm), the regression equation obtained from the wavelength 650 nm was chosen to calculate the concentration of GO suspension.

Table 4. 1 The equations and R^2 values at different wavelength (y is absorbance and x is concentration of GO suspension)

wavelength (nm)	equations	R^2
240	$y = 0.0528x - 0.0901$	0.9911
300	$y = 0.0382x - 0.0591$	0.9922
360	$y = 0.0255x - 0.041$	0.9912
420	$y = 0.0181x - 0.0302$	0.9901
450	$y = 0.0157x - 0.0263$	0.9904
550	$y = 0.0109x - 0.0167$	0.9913
650	$y = 0.0084x - 0.0108$	0.9928

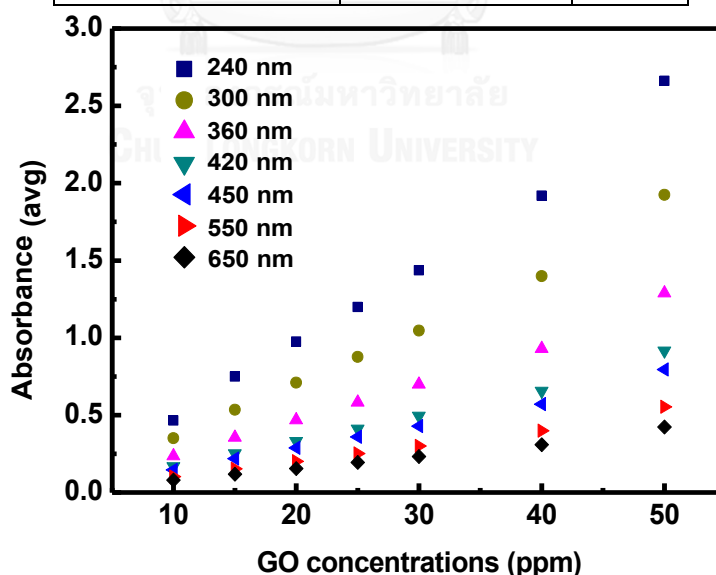


Fig. 4. 10 The calibration curves of the GO concentrations (10-50 ppm) and the average of absorbance at 240, 300, 360, 420, 450, 550 and 650 nm.

To study the dispersion behavior of GO-OAm in organic solvents, the composite of GO-OAm was distributed in different organic solvents; TOL, n-BuOH, i-BuOAc, EtOAc, ACN and EG. The variation of the dispersion behavior might be related to the compatibility of solvents (dipole moments, polarity, and surface tensions as shown in table 4.2) and the hydrophobicity of the GO-OAm [23].

Table 4. 2 The physical properties of DI water and organic solvents [51,52]

Solvents	Polarity index (P')	Dipole moment	Surface tension (mN/m)	Solubility in water (%w/w)	Dielectric constant
DI water	10.2	1.87	72.8	-	80.1
toluene (TOL)	2.4	0.31	28.5	0.051	2.38
n-butanol (nBuOH)	3.9	1.75	24.6	0.43	N.A.
i-butyl acetate (iBuOAc)	4.0	1.84	25.1	7.87	5.01
ethyl acetate (EtOAc)	4.4	1.88	23.8	8.7	6.02
acetonitrile (ACN)	5.8	3.44	19.10	100	37.5
ethylene glycol (EG)	N.A.	2.31	47.7	100	N.A.

*N.A. is not available.

Therefore, the optimization of amount of OAm might be required in order to assess the maximum dispersion of GO in organic solvents. To reach an appropriate amount of OAm used to transfer GO in those solvents, a dispersion activity was defined and calculated as follows:

- 1) The concentration of the dispersed GO in organic solvent using the calibration curve obtained from absorbance at 650 nm

$$A_{650\text{nm}} = 0.0084 C_{\text{GO suspension}} + 0.0108, \text{ where } A_{650\text{nm}} \text{ is absorbance at } 650\text{nm} \text{ and } C_{\text{GO suspension}} \text{ is concentration of GO suspension.}$$

- 2) The re-dispersion of 20 ppm GO suspension in water was used as benchmark; $C'_{\text{GO-suspension (water)}}$.
- 3) The dispersion activity is calculated by ratio of the concentration of re-dispersion of GO suspension in organic solvent and water

$$\text{Dispersion activity} = \frac{C_{\text{GO-suspension (organic solvent)}}}{C'_{\text{GO-suspension (water)}}$$

To optimize amount of OAm used to transfer GO in organic solvents, the weight ratios of GO:OAm were varied at 1:10, 1:50, 1:100, 1:500 and 1:1000, respectively. Fig. 4.11A showed the dispersion activity of GO-OAm using various amount of OAm in several organic solvents. The small index of dispersion activity represented a small proportion of GO that could be transferred to organic solvents. This reflects an insufficient of OAm for transferring GO to organic solvents. However, the high value of the dispersion activity with a large variation was observed when the larger amount of OAm was used. This observation might be originated from an excess amount of OAm. An excess OAm might induced the aggregation/agglomeration of GO to form a multilayer GO nanosheets because the hydrophobicity of long chain hydrocarbon on OAm molecules [23]. Therefore, a suitable amount of OAm should be determined by giving dispersion activity of GO-OAm close to 1 with less variation. This mean the dispersion behavior of GO-OAm in organic solvents is similar to the starting GO suspensions in aqueous solution. In each organic solvent, an appropriate amount of OAm was determined (marking with star symbol). The inset images of fig. 4.11C displayed the digital photographs of the dispersed GO-OAm taken in several organic solvents immediately after the sonication. The DI water was added in order to separate organic phase and aqueous phase. In case of ACN and EG, these solvents are miscible-water solvents.

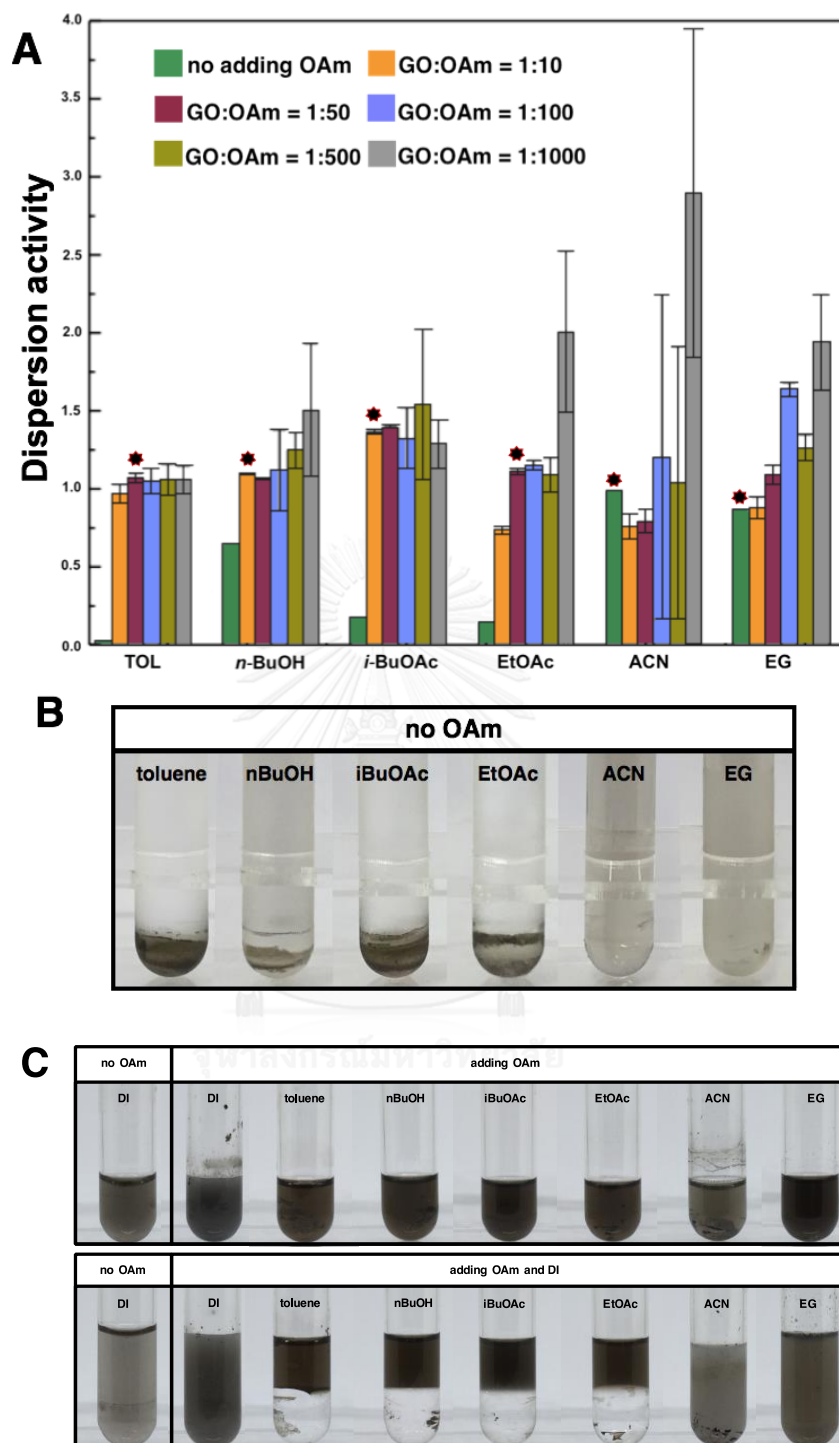


Fig. 4. 11 (A) The chart of the dispersion activity at various weight ratio of GO-OAm in several organic solvents, (B) The dispersed GO in organic solvents and (C) Insets images represent the GO-OAm in organic solvents after sonication, after adding DI water and after adding various amount OAm.

FT-IR spectral analysis was utilized to observe the strong interactions between GO and OAm (GO-OAm) as shown in fig 4.12. The set of characteristic peaks of GO represented at $\sim 3250\text{ cm}^{-1}$ (O-H stretching vibrations), at 1720 cm^{-1} (C=O stretching vibrations), at $\sim 1610\text{ cm}^{-1}$ (aromatic C=C stretching vibrations), and at $\sim 1070\text{ cm}^{-1}$ (C-O-C stretching vibrations). The FT-IR spectra of OAm and GO-OAm showed the strong intensity absorption band at $\sim 2920\text{ cm}^{-1}$ and 2850 cm^{-1} corresponding to the C-H aliphatic stretching vibrations and the C-H bending at $\sim 1465\text{ cm}^{-1}$ [23,57]. Furthermore, we observed the shift of the C=O stretching peak of GO-OAm. These observations confirmed the interaction between amine group of OAm with the functional groups on GO nanosheets.

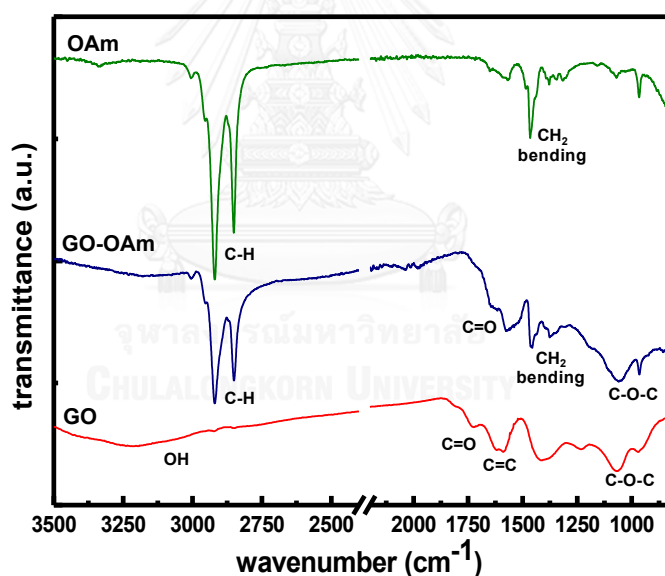


Fig. 4. 12 FT-IR spectra of the original GO suspension, the pure OAm and the GO-OAm.

To examine the stability of the dispersed GO-OAm in organic solvents, the digital images were again taken in the range of 0 – 18 hours after sonication as shown in fig. 4.13. The GO-OAm using an appropriate amount of OAm shows the dispersion with good stability in all organic solvents: TOL, n-BuOH, i-BuOAc, EtOAc, ACN and EG.

The water was added in order to separate organic phase and water phase. In case of ACN and EG, these solvents are homogeneously soluble with water. The long-term stability was examined by leaving the suspensions undisturbed for 18 hours. The results clearly displayed that the starting GO suspensions were completely not dispersed in any organic solvents, while GO-OAm retained its excellent dispersibility in especially n-BuOH, i-BuOAc, EtOAc for at least 6 hours. In case of TOL, a precipitation of GO-OAm was observed after 2 hours. The long-term stability of the GO-OAm might be majorly related to the polarity of the solvents, which TOL provides the lowest polarity in the case. It is worth mentioning that the stability of the dispersion GO-OAm for 6 hours might be adequate for the industrial and research applications. Furthermore, the GO-OAm was easily re-dispersed by bath sonication which is practically use in the real industrial/manufacturing.

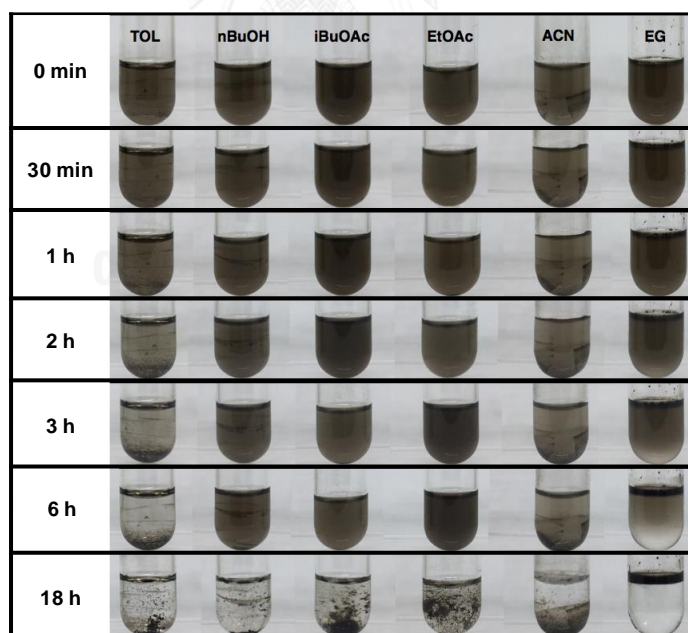


Fig. 4. 13 Inset digital images of the dispersed GO-OAm in several organic solvents immediately after sonication and after leaving for 0-18 hours.

4.3 Phase transferring GO/AgNP composites to organic solvents

The transferring process for GO by using OAm as transferring agent was performed with the GO/AgNP composites. The optimized amount of OAm in each organic solvent was used to increase hydrophobicity of GO surface of the GO/AgNP composites and produce the GO/AgNPs-OAm. The presence of AgNPs on the GO/AgNPs-OAm in the organic solvents was investigated by UV-Visible spectroscopy as shown in fig. 4.14A. It was found that the characteristic Plasmon bands of AgNPs at ~430 nm is clearly detected in all solvents. It should be noted that the dispersive efficiency of the GO/AgNPs-OAm might be different due to the solvent properties. This causes on the variation of baseline shifts in UV-Visible spectra. To eliminate the influences of baseline shifts in the spectra, the normalized UV-Visible spectra was again plotted as shown in fig. 4.14B. It was found that they are very similar suggesting that the level of AgNPs deposited on the GO nanosheets are comparable. This reveals that the GO/AgNP-OAm could be transferred into a wide range of the organic solvents with equally efficiency. In addition, the digital images of the GO/AgNPs-OAm suspension in the organic solvents are shown in fig. 4.14C. From the digital images, they are observed that the GO/AgNPs-OAm is well-dispersed in all organic solvents. To evaluate the stability of the dispersion of the GO/AgNPs-OAm, the suspension solution was monitored undisturbed for 18 hours by capturing the images as shown in fig. 4.14D. From fig. 4.14D, the long-term stability of GO/AgNPs-OAm was observed in especially iBuOAc, EtOAc and EG for at least 6 hours.

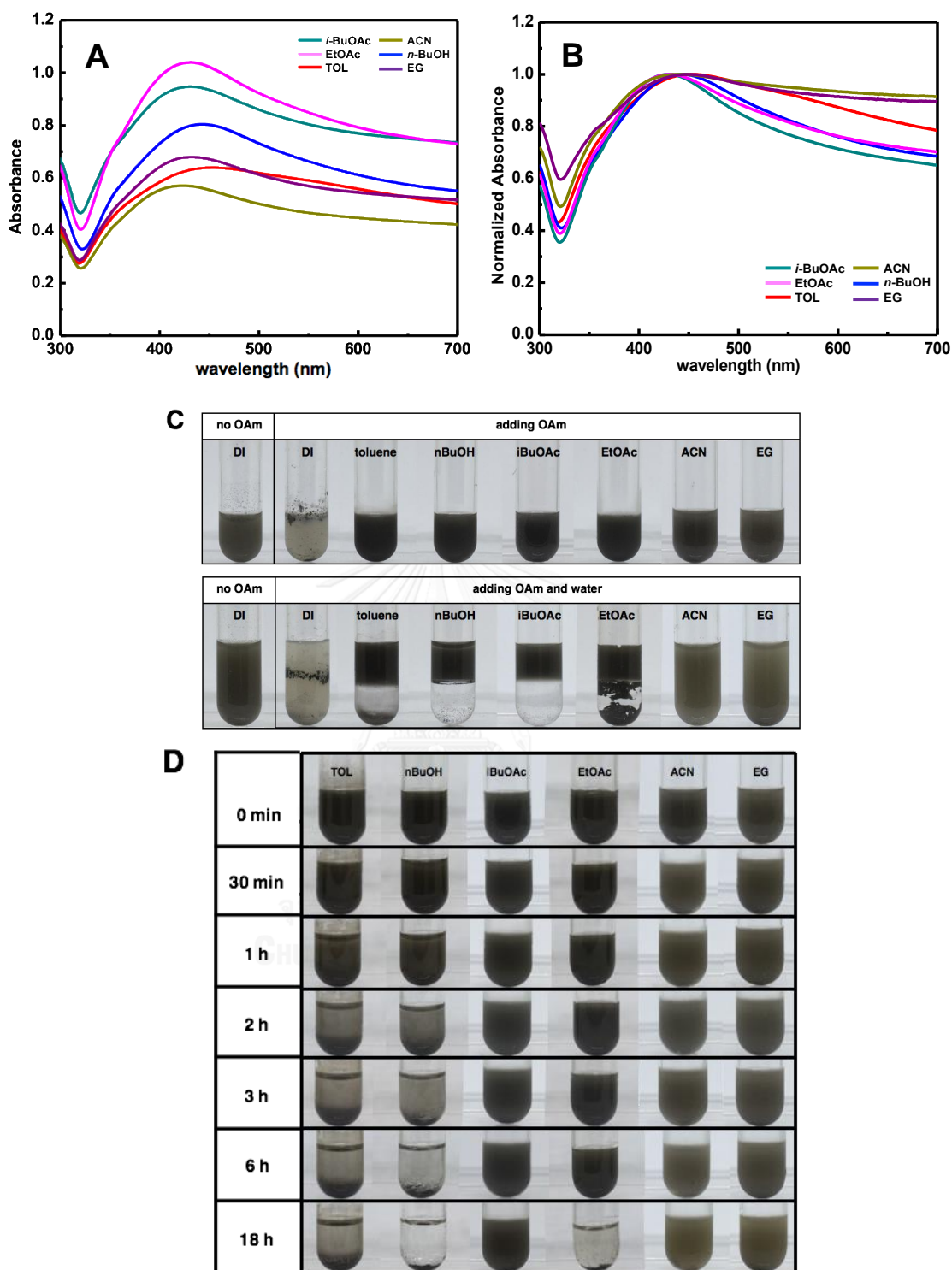


Fig. 4. 14 (A) UV-Visible spectra and (B) normalized UV-visible spectra of the dispersion of GO/AgNPs-OAm in the organic solvents (TOL, *n*-BuOH, *i*-BuOAc, EtOAc and ACN). (C) the digital images represent the dispersed GO/AgNPs-OAm in the organic solvents immediately after sonication, after adding DI water and (D) after leaving them for 0-18 hours.

To examine the decomposition profiles of GO-OAm and GO/AgNPs-OAm were assessed by the thermal gravimetric analysis (TGA) under N₂ environment. Fig. 4.15 showed the TGA thermograms of weight loss as a function of temperature. TGA analysis curves of GO-OAm and GO/AgNPs-OAm were also observed the weight loss profiles at 350-450 °C corresponding to the desorption of the range of C₁-C₃ hydrocarbon fragments. These fragments were referred to amine fragments; C₁NH₂⁺ and C₂NH₂⁺ of the OAm molecules [57,58]. The anchoring amount of AgNPs on the GO nanosheets was approximately 35 wt% comparing to the GO-OAm.

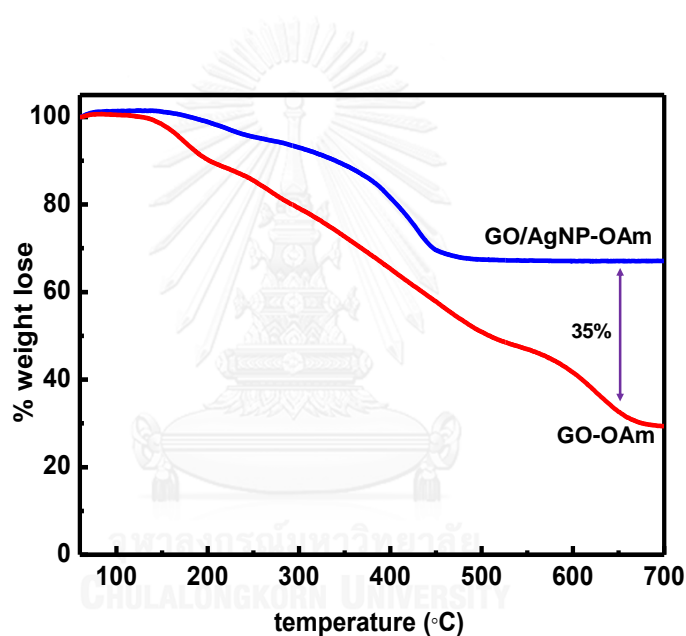


Fig. 4. 15 TGA thermograms of the GO-OAm composites (red line) and the GO/AgNPs-OAm (blue line).

As the results shown above, the GO/AgNPs-OAm was successfully synthesized with high stability and AgNPs are still strongly attached on GO nanosheets after the transferring process. To assess the morphology, the GO/AgNP composites after modifying with OAm in EtOAc was investigated by TEM as shown in fig. 4.16 (A, B). It can be seen that the AgNPs remain on GO nanosheets after transferring to the organic

solvent. However, these particles seem to be disaggregated with the unfolding of GO nanosheets. The unfolding mechanism of GO sheets might be induced by the increasing of the hydrophobicity of GO nanosheets from long hydrocarbon chain of OAm. This enhances the compatibility of modified GO nanosheets with organic media. The average size of AgNPs was approximately 60 nm counted from 100 individual particles (fig. 4.16C).

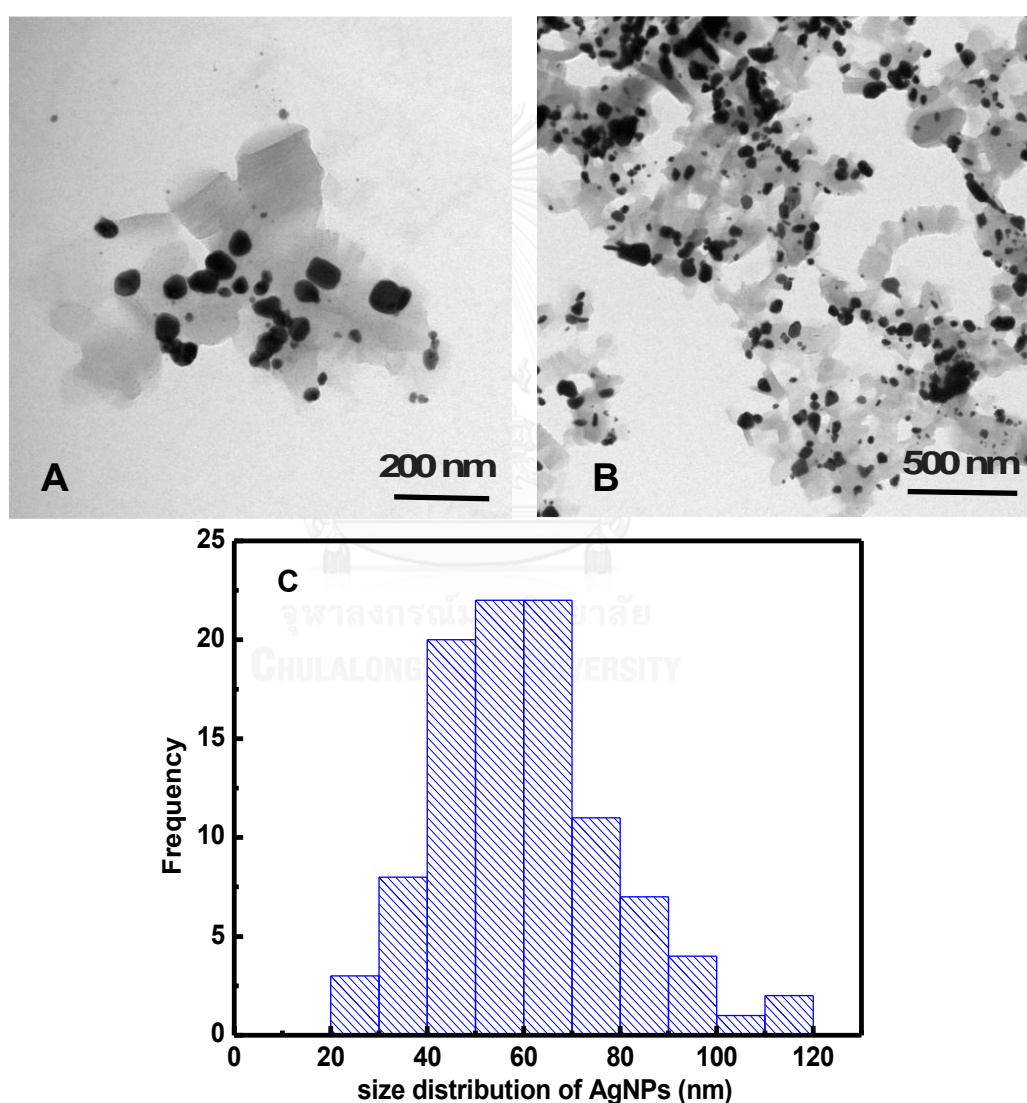


Fig. 4. 16 (A,B) TEM images of GO/AgNPs-OAm in EtOAc (C) histogram of the size distribution of AgNPs on GO nanosheets in EtOAc.

From the observation on TEM images, AgNPs might detach from an unfolded GO nanosheets. To test the stability of the AgNPs deposited on the transferred GO/AgNPs-OAm, the suspension of GO/AgNPs-OAm in organic solvents was sonicated and then followed by centrifuging at 2,000 rpm for 10 min. The supernatant was collected for analyzing while the sediment pellets were re-dispersed in the organic solvents. These two fractions were analyzed by UV-Vis spectroscopy. Fig. 4.17 shows UV-Vis spectra of the supernatant (dot lines) and re-dispersed GO/AgNPs-OAm (solid line). It can be seen that the absorbance of supernatant was mostly lower than the re-dispersed GO/AgNPs-OAm in TOL, n-BuOH, i-BuOAc, EtOAc and ACN. These observations suggest that AgNPs were still remained on GO sheets. However, the Plasmon band of AgNPs (~ 430 nm) was observed in the the supernatant from n-BuOH, EtOAc and i-BuOAc. This suggests that the fractional AgNPs on the GO/AgNPs-OAm were detached.

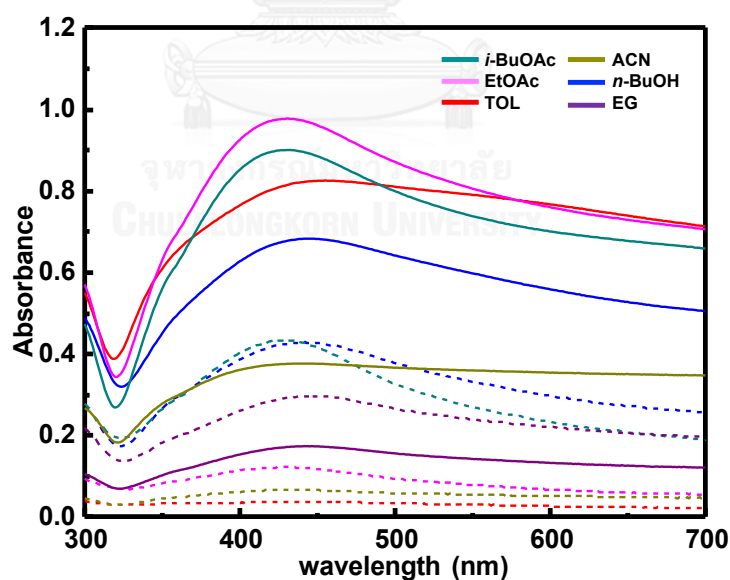


Fig. 4. 17 UV-Vis spectra of the re-dispersed GO/AgNPs-OAm pellets (solid lines) and the supernatant (dot lines) in the organic solvents: TOL, n-BuOH, i-BuOAc, EtOAc and ACN.

To examine the re-dispersion of GO/AgNPs-OAm in organic solvents, the dispersed GO/AgNPs-OAm was left undisturbed for 18 hours. After that, the GO/AgNPs-OAm was re-dispersed again by sonication for 30 min. From the digital images in fig 4.18, the GO/AgNPs-OAm could be easily re-dispersed by sonication without any losing in the dispersive efficiency.

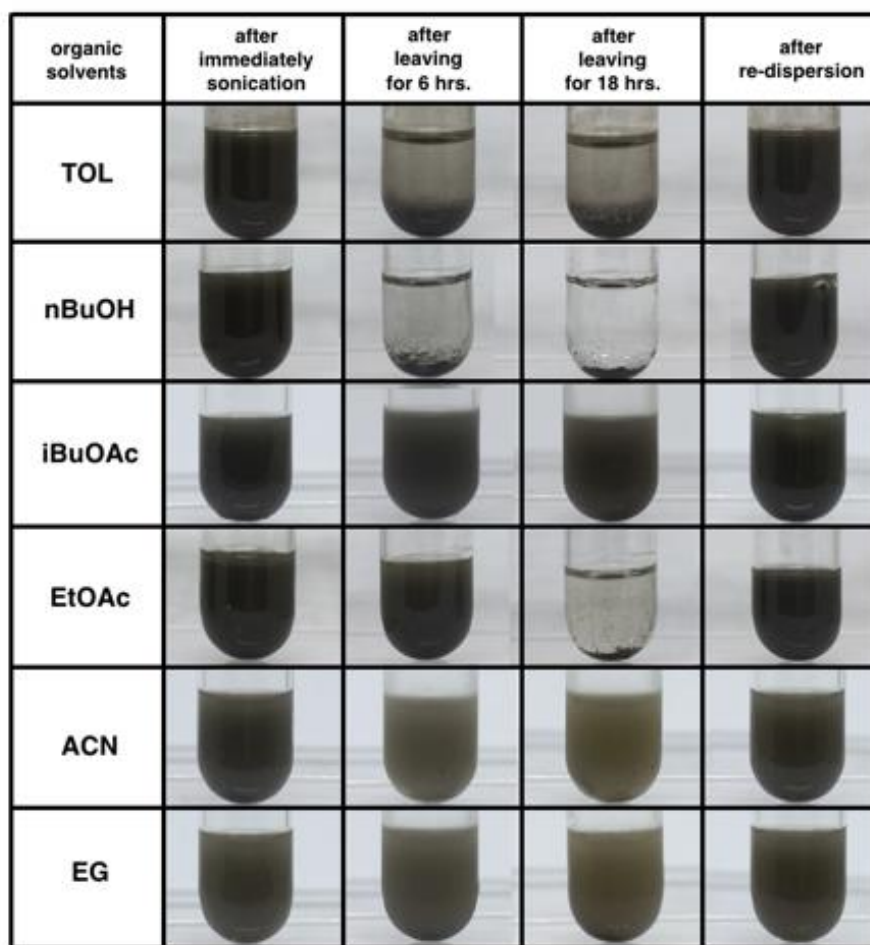


Fig. 4. 18 Inset images of the dispersed GO/AgNPs-OAm in organic solvents after immediately sonication, leaving for 6 hours, 18 hours and after re-dispersion.

CHAPTER 5

CONCLUSIONS

Generally, AgNPs were synthesized through the chemical reduction of silver ions (Ag^+) and reducing agents in aqueous solution. However, some specific application such as coating materials, biosensors and catalyst may call for to transfer the AgNPs into organic solvents. The direct synthesized AgNPs in organic solvent is complicated, costly and low stability.

In this work, we focus on the phase transferring AgNPs in organic solvents by using GO as a carrier material. GO is the one of cruel materials in polymer industry due to its characteristics which differ from graphene. Especially, the existence of the tremendous oxygen-functional groups on GO surface that means GO is easily functionalized for desire applications. As well as, the structure of GO surface is flat single-layered which utilizes to be a great carrier material. Therefore, GO can be a good candidate for deposition of AgNPs on its surface. The methodology carries out two steps; the formation of AgNPs on GO surface through chemical reaction by using DMF as a reducing agent, and then the graphene oxide-silver nanoparticle (GO/AgNP) composites are modified its surface by oleylamine (OAm) in order to improve hydrophobic property for the stable dispersion in organic solvents e.g. toluene, n-butanol, iso-butyl acetate, ethyl acetate, acetonitrile and ethylene glycol. UV-Visible spectroscopy, Fourier-transform Infrared (FTIR) spectra, Raman spectroscopy, X-ray powder diffraction, transmission electron microscopy (TEM), scanning electron microscope (SEM) and energy-dispersive X-ray spectroscopy (EDX) are used to characterized the GO/AgNP composite. The results demonstrate that the AgNPs are uniformly generated and assembled on a surface of GO sheets and the modified GO/AgNP composites is highly dispersed in organic solvents at least 6 hours.

REFERENCES

1. Neumann, C. C. M.; Laborda, E.; Tschulik, K.; Ward, K. R.; Compton, R. G., Performance of silver nanoparticles in the catalysis of the oxygen reduction reaction in neutral media: Efficiency limitation due to hydrogen peroxide escape. *Nano Research* **2013**, *6* (7), 511-524.
2. Alshehri, A. H.; Jakubowska, M.; Młotkowiak, A.; Horaczek, M.; Rudka, D.; Free, C.; Carey, J. D., Enhanced Electrical Conductivity of Silver Nanoparticles for High Frequency Electronic Applications. *ACS Applied Materials & Interfaces* **2012**, *4* (12), 7007-7010.
3. Pandey, S.; Goswami, G. K.; Nanda, K. K., Green synthesis of biopolymer-silver nanoparticle nanocomposite: An optical sensor for ammonia detection. *International Journal of Biological Macromolecules* **2012**, *51* (4), 583-589.
4. Guzman, M.; Dille, J.; Godet, S., Synthesis and antibacterial activity of silver nanoparticles against gram-positive and gram-negative bacteria. *Nanomedicine: Nanotechnology, Biology and Medicine* **2012**, *8* (1), 37-45.
5. Iravani, S.; Korbekandi, H.; Mirmohammadi, S. V.; Zolfaghari, B., Synthesis of silver nanoparticles: chemical, physical and biological methods. *Research in Pharmaceutical Sciences* **2014**, *9* (6), 385-406.
6. Panáček, A.; Kvítek, L.; Pucek, R.; Kolář, M.; Večeřová, R.; Pizúrová, N.; Sharma, V. K.; Nevěčná, T.; Zbořil, R., Silver Colloid Nanoparticles: Synthesis, Characterization and Their Antibacterial Activity. *Journal of Physical Chemistry B* **2006**, *110*, 16248-16253.
7. Wang, H.; Qiao, X.; Chen, J.; Ding, S., Preparation of silver nanoparticles by chemical reduction method. *Colloids and Surfaces A: Physicochemical and Engineering Aspects* **2005**, *256* (2-3), 111-115.
8. Agnihotri, S.; Mukherji, S.; Mukherji, S., Size-controlled silver nanoparticles synthesized over the range 5-100 nm using the same protocol and their antibacterial

- efficacy. *RSC Advances* **2014**, *4* (8), 3974-3983.
9. Bastús, N. G.; Merkoçi, F.; Piella, J.; Puntès, V., Synthesis of Highly Monodisperse Citrate-Stabilized Silver Nanoparticles of up to 200 nm: Kinetic Control and Catalytic Properties. *Chemistry of Materials*. **2014**, *26* (9), 2836-2846.
 10. Dondi, R.; Su, W.; Griffith, G. A.; Clark, G.; Burley, G. A., Highly Size- and Shape-Controlled Synthesis of Silver Nanoparticles via a Templated Tollens Reaction. *Small* **2012**, *8* (5), 770-776.
 11. Jiang, C.; Li, L.; Pong, P. W. T., Controlled convective self-assembly of silver nanoparticles in volatile organic solvent and its application in electronics. *RSC Advances* **2015**, *5* (120), 98747-98756.
 12. Lu, L.; An, X., Silver nanoparticles synthesis using H₂ as reducing agent in toluene-supercritical CO₂ microemulsion. *The Journal of Supercritical Fluids* **2015**, *99*, 29-37.
 13. Zhang, W.; Qiao, X.; Chen, J.; Wang, H., Preparation of silver nanoparticles in water-in-oil AOT reverse micelles. *Journal of Colloid and Interface Science* **2006**, *302* (1), 370-373.
 14. Wang, X.; Xu, S.; Zhou, J.; Xu, W., A rapid phase transfer method for nanoparticles using alkylamine stabilizers. *Journal of Colloid and Interface Science* **2010**, *348* (1), 24-28.
 15. Soliman, M. G.; Pelaz, B.; Parak, W. J.; del Pino, P., Phase Transfer and Polymer Coating Methods Toward Improving the Stability of Metallic Nanoparticles for Biological Applications. *Chemistry of Materials* **2015**, *27* (3), 990-997.
 16. Zhao, S.-Y.; Chen, S.-H.; Li, D.-G.; Yang, X.-G.; Ma, H.-Y., A convenient phase transfer route for Ag nanoparticles. *Physica E: Low-dimensional Systems and Nanostructures* **2004**, *23* (1-2), 92-96.
 17. Joshi, C. P.; Bigioni, T. P., Model for the Phase Transfer of Nanoparticles Using Ionic Surfactants. *Langmuir* **2014**, *30* (46), 13837-13843.

18. Liu, L.; Kelly, T. L., Phase Transfer of Triangular Silver Nanoprisms from Aqueous to Organic Solvent by an Amide Coupling Reaction. *Langmuir* **2013**, *29* (23), 7052-7060.
19. Li, J.; Zeng, X.; Ren, T.; van der Heide, E., The Preparation of Graphene Oxide and Its Derivatives and Their Application in Bio-Tribological Systems. *Lubricants* **2014**, *2* (3), 137-161.
20. Pavlidis, I. V.; Patila, M.; Bornscheuer, U. T.; Gournis, D.; Stamatis, H., Graphene-based nanobiocatalytic systems: recent advances and future prospects. *Trends in Biotechnology* **2014**, *32* (6), 312-320.
21. Jang, J.; Pham, V. H.; Rajagopalan, B.; Hur, S. H.; Chung, J. S., Effects of the alkylamine functionalization of graphene oxide on the properties of polystyrene nanocomposites. *Nanoscale Research Letters* **2014**, *9* (1), 265.
22. Choudhary, S.; Mungse, H. P.; Khatri, O. P., Dispersion of alkylated graphene in organic solvents and its potential for lubrication applications. *Journal of Materials Chemistry* **2012**, *22* (39), 21032-21039.
23. Yu, W.; Xie, H.; Wang, X.; Wang, X., Highly Efficient Method for Preparing Homogeneous and Stable Colloids Containing Graphene Oxide. *Nanoscale Research Letters* **2011**, *6* (1), 47.
24. Kim, J. D.; Palani, T.; Kumar, M. R.; Lee, S.; Choi, H. C., Preparation of reusable Ag-decorated graphene oxide catalysts for decarboxylative cycloaddition. *Journal of Materials Chemistry* **2012**, *22* (38), 20665-20670.
25. Ayan-Varela, M.; Fernandez-Merino, M. J.; Paredes, J. I.; Villar-Rodil, S.; Fernandez-Sanchez, C.; Guardia, L.; Martinez-Alonso, A.; Tascon, J. M. D., Highly efficient silver-assisted reduction of graphene oxide dispersions at room temperature: mechanism, and catalytic and electrochemical performance of the resulting hybrids. *Journal of Materials Chemistry A* **2014**, *2* (20), 7295-7305.
26. Zhang, Y.; Liu, S.; Wang, L.; Qin, X.; Tian, J.; Lu, W.; Chang, G.; Sun, X., One-pot green synthesis of Ag nanoparticles-graphene nanocomposites and their applications in

- SERS, H₂O₂, and glucose sensing. *RSC Advances* **2012**, *2* (2), 538-545.
27. Wang, Y.; Zhen, S. J.; Zhang, Y.; Li, Y. F.; Huang, C. Z., Facile Fabrication of Metal Nanoparticle/Graphene Oxide Hybrids: A New Strategy to Directly Illuminate Graphene for Optical Imaging. *The Journal of Physical Chemistry C* **2011**, *115* (26), 12815-12821.
28. Das, M. R.; Sarma, R. K.; Saikia, R.; Kale, V. S.; Shelke, M. V.; Sengupta, P., Synthesis of silver nanoparticles in an aqueous suspension of graphene oxide sheets and its antimicrobial activity. *Colloids and Surfaces B: Biointerfaces* **2011**, *83* (1), 16-22.
29. Chook, S. W.; Chia, C. H.; Zakaria, S.; Ayob, M. K.; Chee, K. L.; Huang, N. M.; Neoh, H. M.; Lim, H. N.; Jamal, R.; Rahman, R., Antibacterial performance of Ag nanoparticles and AgGO nanocomposites prepared via rapid microwave-assisted synthesis method. *Nanoscale Research Letters* **2012**, *7* (1), 1-7.
30. Liu, H.; Zhong, L.; Yun, K.; Samal, M., Synthesis, characterization, and antibacterial properties of silver nanoparticles-graphene and graphene oxide composites. *Biotechnology and Bioprocess Engineering* **2016**, *21* (1), 1-18.
31. Shao, W.; Liu, X.; Min, H.; Dong, G.; Feng, Q.; Zuo, S., Preparation, characterization, and antibacterial activity of silver nanoparticle-decorated graphene oxide nanocomposite. *ACS Applied Materials and Interfaces* **2015**, *7* (12), 6966-6973.
32. Cui, J.; Yang, Y.; Zheng, M.; Liu, Y.; Xiao, Y.; Lei, B.; Chen, W., Facile fabrication of graphene oxide loaded with silver nanoparticles as antifungal materials. *Materials Research Express* **2014**, *1* (4), 045007.
33. Tang, J.; Chen, Q.; Xu, L.; Zhang, S.; Feng, L.; Cheng, L.; Xu, H.; Liu, Z.; Peng, R., Graphene oxide-silver nanocomposite as a highly effective antibacterial agent with species-specific mechanisms. *ACS Applied Material and Interfaces* **2013**, *5* (9), 3867-3874.
34. de Faria, A. F.; Perreault, F.; Shaulsky, E.; Arias Chavez, L. H.; Elimelech, M., Antimicrobial Electrospun Biopolymer Nanofiber Mats Functionalized with Graphene Oxide-Silver Nanocomposites. *ACS Applied Material and Interfaces* **2015**, *7* (23),

12751-12759.

35. Vijay Kumar, S.; Huang, N. M.; Lim, H. N.; Marlinda, A. R.; Harrison, I.; Chia, C. H., One-step size-controlled synthesis of functional graphene oxide/silver nanocomposites at room temperature. *Chemical Engineering Journal* **2013**, *219*, 217-224.
36. Liu, S.; Tian, J.; Wang, L.; Sun, X., Microwave-assisted rapid synthesis of Ag nanoparticles/graphene nanosheet composites and their application for hydrogen peroxide detection. *Journal of Nanoparticle Research* **2011**, *13* (10), 4539-4548.
37. Shen, J.; Shi, M.; Li, N.; Yan, B.; Ma, H.; Hu, Y.; Ye, M., Facile synthesis and application of Ag-chemically converted graphene nanocomposite. *Nano Research* **2010**, *3* (5), 339-349.
38. Zhou, X.; Huang, X.; Qi, X.; Wu, S.; Xue, C.; Boey, F. Y. C.; Yan, Q.; Chen, P.; Zhang, H., In Situ Synthesis of Metal Nanoparticles on Single-Layer Graphene Oxide and Reduced Graphene Oxide Surfaces. *The Journal of Physical Chemistry C* **2009**, *113* (25), 10842-10846.
39. Cobley, C. M.; Chen, J.; Cho, E. C.; Wang, L. V.; Xia, Y., Gold nanostructures: a class of multifunctional materials for biomedical applications. *Chemical Society Reviews* **2011**, *40* (1), 44-56.
40. Xiu, Z.-m.; Zhang, Q.-b.; Puppala, H. L.; Colvin, V. L.; Alvarez, P. J. J., Negligible Particle-Specific Antibacterial Activity of Silver Nanoparticles. *Nano Letters* **2012**, *12* (8), 4271-4275.
41. Yang, J.; Lee, J. Y.; Ying, J. Y., Phase transfer and its applications in nanotechnology. *Chemical Society Reviews* **2011**, *40* (3), 1672-1696.
42. Gao, W., Graphene Oxide Reduction Recipes, Spectroscopy, and Applications. **2015**.
43. Pavlidis, I. V.; Patila, M.; Bornscheuer, U. T.; Gournis, D.; Stamatis, H., Graphene-based nanobiocatalytic systems: recent advances and future prospects. *Trends in Biotechnology* **2014**, *32* (6), 312-320.
44. Moazzami Gudarzi, M., Enhancement of dispersion and bonding of graphene-polymer through wet transfer of functionalized graphene oxide. *Express Polymer*

- Letters* **2012**, *6* (12), 1017-1031.
45. Xue, Y.; Liu, Y.; Lu, F.; Qu, J.; Chen, H.; Dai, L., Functionalization of Graphene Oxide with Polyhedral Oligomeric Silsesquioxane (POSS) for Multifunctional Applications. *The Journal of Physical Chemistry Letters* **2012**, *3* (12), 1607-1612.
 46. Fu, W. L.; Zhen, S. J.; Huang, C. Z., Controllable preparation of graphene oxide/metal nanoparticle hybrids as surface-enhanced Raman scattering substrates for 6-mercaptopurine detection. *RSC Advances* **2014**, *4* (31), 16327-16332.
 47. Lee, J.; Novoselov, K. S.; Shin, H. S., Interaction between Metal and Graphene: Dependence on the Layer Number of Graphene. *ACS Nano* **2011**, *5* (1), 608-612.
 48. Lu, G.; Mao, S.; Park, S.; Ruoff, R. S.; Chen, J., Facile, noncovalent decoration of graphene oxide sheets with nanocrystals. *Nano Research* **2009**, *2* (3), 192-200.
 49. Manolata Devi, M.; Sahu, S. R.; Mukherjee, P.; Sen, P.; Biswas, K., Graphene–Metal Nanoparticle Hybrids: Electronic Interaction Between Graphene and Nano-particles. *Transactions of the Indian Institute of Metals* **2016**, *69* (4), 839-844.
 50. Iravani, S.; Korbekandi, H.; Mirmohammadi, S. V.; Zolfaghari, B., Synthesis of silver nanoparticles: chemical, physical and biological methods. *Research in Pharmaceutical Sciences* **2014**, *9* (6), 385-406.
 51. Smallwood., M., I. *Handbook of organic solvent properties*. **1996**.
 52. Louisiana State University Macromolecular Studies Group server. <http://macro.lsu.edu/howto/solvents.htm> (accessed November 13, 2016)
 53. Pastoriza-Santos, I.; Liz-Marzán, L. M., *N, N'*-Dimethylformamide as a Reaction Medium for Metal Nanoparticle Synthesis. *Advanced Functional Materials* **2009**, *19* (5), 679-688.
 54. Shafeeyan, M. S.; Daud, W. M. A. W.; Houshmand, A.; Shamiri, A., A review on surface modification of activated carbon for carbon dioxide adsorption. *Journal of Analytical and Applied Pyrolysis* **2010**, *89* (2), 143-151.
 55. Huang, Y.-F.; Wu, D.-Y.; Zhu, H.-P.; Zhao, L.-B.; Liu, G.-K.; Ren, B.; Tian, Z.-Q., Surface-enhanced Raman spectroscopic study of p-aminothiophenol. *Physical Chemistry*

Chemical Physics **2012**, *14* (24), 8485-8497.

56. Manard, M. J.; Kemper, P. R.; Bowers, M. T., Binding interactions of mono- and diatomic silver cations with small alkenes: experiment and theory. *International Journal of Mass Spectrometry* **2005**, *241* (2–3), 109-117.
57. Shi, Y.-y.; Sun, B.; Zhou, Z.; Wu, Y.-t.; Zhu, M.-f., Size-controlled and large-scale synthesis of organic-soluble Ag nanocrystals in water and their formation mechanism. *Progress in Natural Science: Materials International* **2011**, *21* (6), 447-454.
58. Humphrey, J. J. L.; Sadasivan, S.; Plana, D.; Celorrio, V.; Tooze, R. A.; Fermín, D. J., Surface Activation of Pt Nanoparticles Synthesised by “Hot Injection” in the Presence of Oleylamine. *Chemistry – A European Journal* **2015**, *21* (36), 12694-12701.
59. Khan, M.; Tahir, M. N.; Adil, S. F.; Khan, H. U.; Siddiqui, M. R. H.; Al-warthan, A. A.; Tremel, W., Graphene based metal and metal oxide nanocomposites: synthesis, properties and their applications. *Journal of Materials Chemistry A* **2015**, *3* (37), 18753-18808.

VITA

Name: Miss Oraporn Wong-u-ra

Date of Birth: 10 June 1991

Birth place: Nakhonphanom, Thailand

Contact Address: 411/67 U-delight condo, Pracha-utid RD.

Huaykwang, Bangkok 10310, Thailand

E-mail: oraporn.w@gmail.com

Education:

2014 B.Sc. Chemistry, Faculty of Science,

Chulalongkorn University, Thailand

2017 M. Sc. Petrochemistry and Polymer Science Program,

Faculty of Science, Chulalongkorn University, Thailand

Conferences:

February 9-1, 2016 Pure and Applied Chemistry International

Conference 2016, Thailand.

November 30, December 1-2, 2016 The 42nd Congress on Science

and Technology of Thailand.

Proceeding:

Wong- u- ra O. ; Ekgasit, S. ; Wongravee, K. , Highly dispersed graphene oxide/silver nanoparticle (GO/AgNP) composites in organic solvents, Proceedings of the 42nd Congress on Science and Technology of Thailand (STT 42), Bangkok, Thailand.

